Study of Benzene Hydrogenation over Ni/Al_2O_3 Catalyst in a Fixed Bed Reactor

Thesis Submitted in the Fulfilment of the Requirement
of Master of Chemical Engineering

by

Arijit Saha
Class Roll No. 002210302001
Examination Roll No. M4CHE24001
Registration No. 163435 of 2022- 2023

Under the supervision of

Dr. Shyamal Roy
Assistant Professor
CHEMICAL ENGINEERING DEPARTMENT
JADAVPUR UNIVERSITY
KOLKATA-700032

2024

CERTIFICATE

This is to certify that **Mr. Arijit Saha**, Final year Masters of Chemical Engineering (M.ChE) examination student of Department of Chemical Engineering, Jadavpur University, **Class Roll No. 002210302001, Registration No. 163435 of 2022-2023, Examination Roll No. M4CHE24001,** has completed the Project work titled, "The study of hydrogenation of benzene on alumina supported nickel catalyst" under the guidance of Dr. Shyamal Roy during his Master's Curriculum. This work has not been reported earlier anywhere and can be approved for submission in partial fulfillment of the course work.

Pdas 30/5/24

Prof. Papita Das
Head of the Department
Chemical Engineering
Department
Jadavpur University
Kolkata-700034

HEAD
CHEMICAL ENGINEERING DEPARTMENT
JADAVPUR UNIVERSITY
Kolkata-700 032

Dipak Laha 30/5/24

Prof. Dipak Laha
Dean
Jadavpur University
Kolkata-700034

DEAN
Faculty of Engineering & Technology
JADAVPUR UNIVERSITY
KOLKATA-700 032

Shyamal Roy
30/05/2024

Dr. Shyamal Roy
M.E. Project Guide & Supervisor
Chemical Engineering
Department
Jadavpur University
Kolkata-700034

Assistant Professor
CHEMICAL ENGINEERING DEPARTMENT
JADAVPUR UNIVERSITY
Kolkata-700 032

ACKNOWLEDGEMENT

I would like to express my sincere gratitude to everyone who contributed significantly to the successful completion of this research paper. Firstly, I acknowledge Dr. Shyamal Roy, Assistant Professor at Jadavpur University, for his invaluable guidance, profound insights, and unwavering support throughout the entire research process. Furthermore, I extend my thanks to Abhishek Siuli, Soumyajit Das, Susmita Maity and Avik Kr. Basu for their collaborative contributions, engaging discussions, and assistance across various aspects of the research.

I would also like to express gratitude to Prof. Papita Das HOD of chemical engineering department, Jadavpur University and other faculties of the Chemical Engineering Department at Jadavpur University

Arijit Sahoo
31/5/2024

.....

Signature of the Candidate

Chemical Engineering Department

Jadavpur University

Kolkata-700032

TABLE OF CONTENETS

Sl. No.	Content		Page No.
1.	**Introduction**		2
	1.1.	Importance of hydrogenation of aromatic compounds	2
	1.2.	Different types of reactors for hydrogenation of benzene	6
	1.3.	Different types of catalyst synthesis methods	7
	1.4.	Different types of catalyst and support materials	13
	1.5.	Advantages of Excess Solution Impregnation Method (ESI)	20
	1.6.	Different types of catalysts and support materials	20
2.	**Literature review**		31
3.	**Experimental procedure**		53
4.	**Result & discussions**		63
	4.1.	Catalyst Characterization	63
	4.1.1.	BET analysis	63
	4.1.2.	TGA analysis	65
	4.2.	Effect of parameters	67
	4.2.1.	Effect of Temperature on Benzene conversion	67
	4.2.2.	Effect of H_2 Pressure on Benzene conversion	69
	4.2.3.	Effect of Feed LHSV on Benzene Conversion	70
	4.3.	Modelling	72
	4.4.	Reaction mechanism of hydrogenation of benzene over (2 wt.%)Ni/γ-Al_2O_3 catalyst	75
5.	**Conclusions & Future work**		78
	5.1.	Conclusions	78
	5.2.	Future Work	80
	References		81
	Appendix A		
	Appendix B		
	Appendix C		
	Bio data		

LIST OF FIGURES

Figure No.	Content	Page No.
Fig.1.	Importance of reactors in benzene hydrogenation reaction	6
Fig.2.	Schematic diagram of packed-bed reactor	8
Fig.3.	Schematic diagram of fluidized bed reactor	9
Fig.4.	Typical slurry-phase hydrocracker	10
Fig.5.	Schematic diagram of batch reactor	11
Fig.6.	Schematic Diagram of membrane reactor	12
Fig.7.	Schematic diagram of precipitation method	14
Fig.8.	Methodology of sol-gel synthesis for metal oxide nanostructure	15
Fig.9.	Effect of potential voltage on functional properties of AZO thin films, prepared by electrodeposition method	16
Fig.10.	Development of atomic layer deposition (ALD) process	17
Fig.11.	Preparation of Ni-W/SiO_2 catalyst by impregnation method	18
Fig.12.	Schematic diagram for chemical vapour deposition method	19
Fig.13.	Pore structure and surface functional groups of activated carbon	27
Fig.14.	Breakup structures of Carbon Nanotubes	28
Fig.15.	a) Structures of graphene nanomaterials and b) Illustration of possible covalent/non-covalent interactions between protein and GO structures	29
Fig.16.	Preparation of (2 wt.%)Ni/γ-Al_2O_3 by ESI method	55
Fig.17.	Schematic diagram of continuous-upflow high pressure and temperature reactor	56
Fig.18.	Steps required for BET analysis	58
Fig.19.	BET analyser	58
Fig.20.	Steps involved in TGA analysis	60

Fig.21.	Thermogravimetric analysis instrument to study the decomposition of a material	60
Fig.22.	N_2 adsorption-desorption isotherm of (2 wt.%)Ni/γ-Al_2O_3	64
Fig.23.	TGA curve of fresh (2 wt.%)Ni/γ-Al_2O_3 catalyst	66
Fig.24.	Influence of temperature on benzene conversion at H_2 pressure=25 bar, feed LHSV = 2 min^{-1}	67
Fig.25.	Arrhenius plot of ln(k) as a function of 1/T for (2 wt.%)Ni/γ-Al_2O_3 catalyst	68
Fig.26.	Influence of H_2 pressure on benzene conversion at temperature = 390^0C, feed LHSV = 2 min^{-1}	70
Fig.27.	Benzene conversion vs LHSV plot at pressure 20 bar and temperature 663 K	71
Fig.28.	Arrhenius plot of ln(k) as a function of 1/T	73
Fig.29.	Estimation of Power Law Model to determine the order of Bz and H_2 at T = 390^0C, feed flow rate = 8 mL/min	73

LIST OF TABLES

Table No.	Content	Page No.
Table 1.	Concentration of benzene, toluene, ethylbenzene and xylene (BTEX) compounds in jet fuel and their solubility, according to Raoult's Law	4
Table 2.	List of some metal oxide support materials and their applications	22
Table 3.	List of bimetallic catalyst with different types of support materials	23
Table 4.	Description of some tri-metallic catalysts	25
Table 5.	Specifications of the BET analyser and operation conditions	59

ABSTRACT

The performance and activity of (2 wt.%)Ni/γ-Al_2O_3 catalyst in the hydrogenation of benzene reaction was studied in a high pressure continuous up-flow catalytic fixed bed reactor. Aluminium oxide (Al_2O_3) was employed as a support material to synthesize (2 wt%)Ni/γ-Al_2O_3 hydrogenation catalyst using excess solution impregnation method (ESI). Two of the characterizations BET and TGA analysis are carried out in this study. The BET surface area of (2 wt.%)Ni/γ-Al_2O_3 using BET analysis gives 24.79 m^2/g and TGA analysis shows an effective thermal stability of the catalyst. Two parameters of the reactor such as pressure and temperature were varied keeping the liquid hourly space velocity (LHSV) = 2 min^{-1} fixed to understand the effect on benzene conversion. It was observed that benzene conversion was increased with increasing H_2 pressure and after that slightly decreases to 25 bar at temperature 390^0C and LHSV = 2 min^{-1}. Further, the benzene conversion is dependent upon temperature and shows a maximum at 330^0C and activation energy around 23.24 kJ/mol. The study also shows the effect of LHSV on benzene conversion at, T=390^0C and P=25 bar. However, Power Law model of hydrogenation of benzene gives a perfect fit on data and it was found that, the order of H_2 is 1 represents a 1^{st} order whereas, the order of benzene is 0.8 (close to 1^{st} order). It was found that (2 wt%)Ni/γ-Al_2O_3 catalyst showed better performance and activity in the hydrogenation of benzene reaction.

ABBREVIATIONS

AC	: Activated Carbon
ALD	: Atomic Layer Deposition
BET	: Brunauer, Emmette and Teller analysis
BTEX	: Benzene, Toluene, ethylbenzene, m,p-xylenes
CNT	: Carbon Nano-tubes
CVD	: Chemical Vapour Deposition
DRIFTS	: Diffuse Reflectance Infrared Fourier Transform Spectroscopy
EDF	: Equilibrium Deposition Filtration
ESI	: Excess Solution Impregnation
ESR	: Ethanol Steam Reforming
HMS	: Hollow Molecular Sieve
HNT	: Halloysite Aluminosilicate Nanotubes
HOB	: Hydrogenation of Benzene
HZSM	: Highly zeolite Socony Mobil
LHSV	: Liquid Hourly Space Velocity
LOGCs	: Liquid Organic Hydrogen Carriers
LOHCs	: Liquid Organic Hydrogen Carriers
MCM	: Mobile Crystalline Material
MKM	: Micro Kinetic Modelling
NDI	: Non-Dry Impregnation
SBA	: Santa Barbara Amorphous Material
SCR	: Selective Catalytic Reduction
SEM	: Scanning Electron Microscopy
TGA	: Thermogravimetric Analysis
TPR	: Temperature Programmed Reduction
WHSV	: Weight Hourly Space Velocity
ZSM	: Zeolite Socony Mobil

DEDICATED TO

MY PARENTS

CHAPTER 1

INTRODUCTION

CHAPTER 1

INTRODUCTION

In the recent years rapid development of industries increases the environmental impact which is harmful for human health and ecological systems. So, the action towards environmental pollution control is a vital task due to its strong mobility and wider aspects of pollution range. Based on the composition of the pollutants, atmospheric contaminants mainly consist of Nitrogen Oxides (NO, N_2O and NO_2), Carbon Monoxides (CO), Particulate matter and Sulphur compounds (H_2S and SO_2) (Yao et al., 2014). Due to the heavy usage of fossil fuel in industries the pollution level simultaneous increases and for that reason researchers are heading towards an alternative approach for energy generation. Hydrogen energy plays an important role in case of alternative energy resource and also considered as a clean, efficient, versatile renewable energy.

1.1. Importance of Hydrogenation of aromatic compounds

Purification step for fossil fuels like petrol, diesel which are basically derived from crude oil can reduces the environment impact. Hydrogenation of benzene is an important part in refineries due to its major environmental regulations for its concentration in petrol or diesel fuel. Larger portion of benzene around 75%-80% entering the motor produces gasoline pool through catalytic reforming process. Subsequently the hydrogenation of fraction reaches in benzene and avoids the heavy consumption of hydrogen which results drastic reduction in octane number for the gasoline pool. After following these routes reformate gasoline containing benzene concentration meets the environmental regulations (Savva et al., 2008). Here, catalytic hydrogenation of petrol or diesel can severely increase the advantageous approach for energy generation with controlling the pollution level. Technically, the

aromatics impart poor ignition quality of diesel and petrol and lower the cetane number of diesel and petrol. Aromatics also increase the smoke point of jet fuel, emission of particulate matters. These particulate matters and aromatics emissions are environmental hazards, and these are known to be responsible for various diseases when inhaled by human beings. Therefore, stringent environmental regulations are being directed to lower these hazardous emissions from vehicle exhaust (Roy et al., 2013). Consequently, this along with growing demand for high-quality diesel and petrol fuels has brought hydrogenation processes to center stage in the modern refinery strategies.

The drawbacks of the conventional hydrogenation process include-Severe operating conditions, high temperature, high pressure, low space velocity, hydrogen to feed mole ratios to achieve efficient aromatic reduction. Conventional hydrogenation process catalysts comprising sulphide mixed oxide (Ni-Mo, Ni-W, and Co-Mo) can only perform moderate levels of aromatic saturation (Al-Attas et al., 2019). Under these systems, increasing operation severity (temperature and pressure) does not result in deep levels of aromatics saturation because of thermodynamic limitations. Currently most of the industries are heading towards hydrogenation process under stringent environmental rules and regulations. The process itself is less harmful for human beings and also for atmosphere as the product is cyclic compound (Zhou et al., 2020). From the environmental perspective one of the main goals is to decrease the amount of benzene presence in reformate diesel and the catalytic hydrogenation is an effective method as compared to others. As we can see from the table that, the concentration of benzene in jet fuel is much lower as compared to other compounds such as toluene, ethylbenzene, m,p-xylenes and o-xylenes. In case of jet fuel, the concentration as well as the effective solubility of BTEX compounds is listed below

Table.1. Concentration of benzene, toluene, ethylbenzene and xylene (BTEX) compounds in jet fuel and their solubility, according to Raoult's Law (Elias, Chang,. 2020).

Compounds	Concentration in jet fuel (mg/L)	Solubility (mg/L)
Benzene	28	0.1315
Toluene	422	0.5065
Ethylbenzene	1198	0.3542
m,p-xylenes	2922	1.7737
o-xylene	2545	2.7661

One of the main reasons for lower concentration of benzene (28 mg/L) in jet fuel is its potential to form harmful emission when burned. Also, benzene is a known carcinogen and the combustion process can produce pollutants which is detrimental for both environment and human health. On the other hand, hydrogenation reaction of benzene is more complex compare to other hydrocarbons due to its unique stability and structure. Other reasons are discussed below.

Since, benzene is an aromatic compound, it possesses highly stable aromatic ring structure with pi electrons. This stability represents the presence of resonance within the ring and gives the planar, hexagonal structure. So, to break the aromaticity requires higher amount of energy input which makes the reaction less favorable. Hydrogenation of benzene often leads to side reactions. Over-hydrogenation or during ring saturation can produce several undesirable by-products such as cyclohexene, cyclohexadienen, methycyclohexane and ethylcyclohexane. Further, benzene is a stable compound and its hydrogenated derivative (cyclohexane) is

typically more thermodynamically stable, which means that benzene is not as thermodynamically favourable. Benzene has higher degree of unsaturation compared to other BTEX compounds such as ethylbenzene, toluene and xylene. Benzene is lack of any aliphatic unsaturation (double or triple bonds) and for which its unsaturation is entirely aromatic. Due to the presence of this unique structure and lavk of double or triple bonds to be directly saturated, different mechanism for hydrogenation is required.

The study focuses on the usage of nickel catalyst supported on Al_2O_3 considering the nickel loading (2 wt.%) to understanding the catalytic activity in case of benzene hydrogenation. Hydrogenation process generally converts aromatics from unsaturated to saturated compounds, so the process basically breaks the double, triple bonds to single bonds. During hydrogenation process of benzene addition of hydrogen atoms convert unsaturated compound benzene into saturated compound cyclohexane. Catalytic hydrogenation of benzene also plays a vital role both in laboratory and industrial research work. Benzene and Cyclohexane are two distinct compounds and possess different properties (Taleb et al., 2023). Benzene is basically an aromatic hydrocarbon due to the presence of double bonds with molecular formula C_6H_6 whereas Cyclohexane is a cyclic hydrocarbon with molecular formula C_6H_{12}. However, Cyclohexane is less toxic than Benzene and exhibits different chemical along with toxological properties. The reason is due to the presence of double bond in benzene and saturated nature of cyclohexane. Due to the presence of alternate single and double bonds in benzene represents a more unstable compound as compare to cyclohexane. The hydrogenation process for the reduction of benzene is generally employed in industries and various applications for different reasons. Reduction of functional groups such as carbonyl group (C=O), alcohol group (C-OH), nitro ($-NO_2$) and amino group ($-NH_2$) are obtained through hydrogenation process (Wang et al., 2023). Moreover, catalytic hydrogenation

process also plays an important role for impurity removal, hydrogenation of alkenes and alkynes, to convert unsaturated compound to saturated.

1.2. Importance of reactor in benzene hydrogenation reaction

Reactors play an important role in hydrogenation reaction whenever a large-scale production is required in an industrial process. There are some reasons which implicates the importance of reactors in hydrogenation reaction. In case of efficiency, reactors help to optimize the efficiency for hydrogenation reaction while providing the necessary conditions such as pressure, temperature and also the effective mixing between reactant and catalyst.

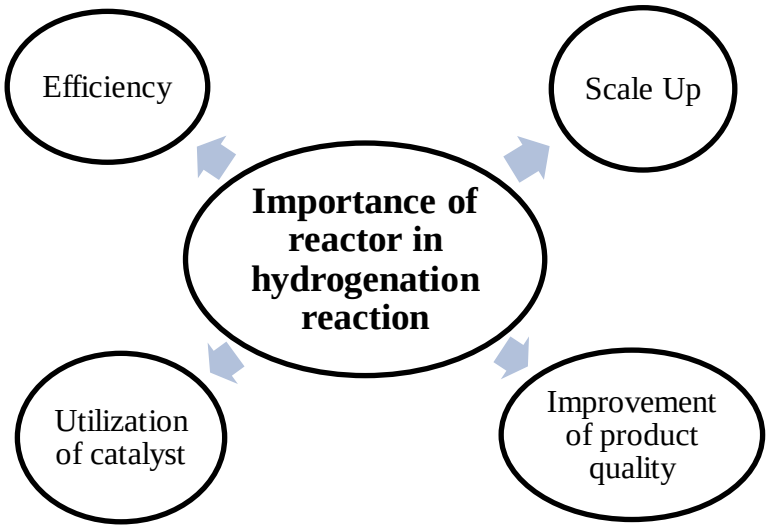


Fig.1. Importance of reactors in benzene hydrogenation reaction

For scaling up reaction reactors play a crucial role in case of scaling up the hydrogenation reaction from laboratory scale to industrial scale. Scale up of reactors also helps to improve the processing of large quantities of reactants while maintain the product quality. Most of the cases catalyst plays a crucial role in order to achieve a desired conversion of reactants. Here, reactors help to optimize the usage of catalysts which plays an important role in hydrogenation reaction. Reactors basically provide the environment where catalyst can

efficiently interact with catalyst including the minimization of cost associated with catalyst consumption. Furthermore, reactors used in hydrogenation reaction impart a crucial role by controlling various parameters like reaction conditions, residence time which is directly connected with the quality of final product (Haut et al., 2004). Here, proper design of reactor as well as operation is required in order to obtain desired purity and product quality.

1.3. Different types of reactors for hydrogenation of benzene

There are different types of reactors that can be used in hydrogenation reaction based on the factors such as scale of production, desired reaction conditions. Some of the descriptions of reactors used in benzene hydrogenation reaction include

1.3.1. Fixed bed reactor

In case of benzene hydrogenation reaction fixed bed reactor is one of the common choices for industrial scale production. This type of reactor is well suited for an effective utilization of catalyst, continuous operation and a good control over reaction conditions. Here, a bed of catalyst is packed inside a cylindrical vessel and catalysts used for benzene hydrogenation reaction are typically metal catalyst supported on a high surface area material like silica or alumina. Common types of metal catalysts include platinum (Pt), palladium (Pd) and nickel (Ni) supported on aluminium oxide (Al_2O_3). Benzene is generally fed into the reactor along with a stream of hydrogen gas. In this type of reactor, to obtain the desired stoichiometry and reaction condition, flow rates of both benzene and hydrogen are controlled in a proper manner. Whenever, feed mixture consist of benzene and hydrogen comes in contact with the catalyst particles, promotes hydrogenation reaction which results in the formation of primary compound cyclohexane collected from the downstream of the reactor.

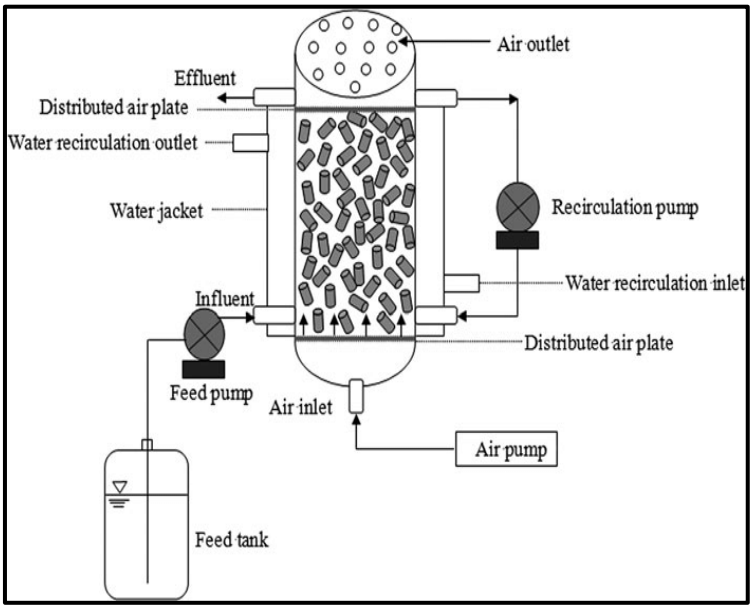


Fig. 2. Schematic diagram of packed-bed reactor (Lin., 2015)

In fixed bed reactor the extent of benzene conversion depends upon various types of factors such as pressure, temperature, residence time and catalyst activity. While, using fixed bed reactor for a long run the activity of catalyst may decreases due to deactivation or fouling. Periodic regeneration of the catalyst is important to restore its activity and to maintain performance of the reactor.

1.3.2. Fluidized bed reactor

In fluidized bed reactor H_2 gas is passed through a bed of catalyst particles, causing them to become suspended in the gas phase medium and behaves like a fluid. This phenomenon promotes an excellent heat transfer as well as mixing, which leads to an uniform distribution of temperature within the reactor and enhanced the reaction rate. In case of uniform temperature distribution during hydrogenation reaction of benzene, hot spots are prevented within the reactor and minimize the side reactions while improving the selectivity.

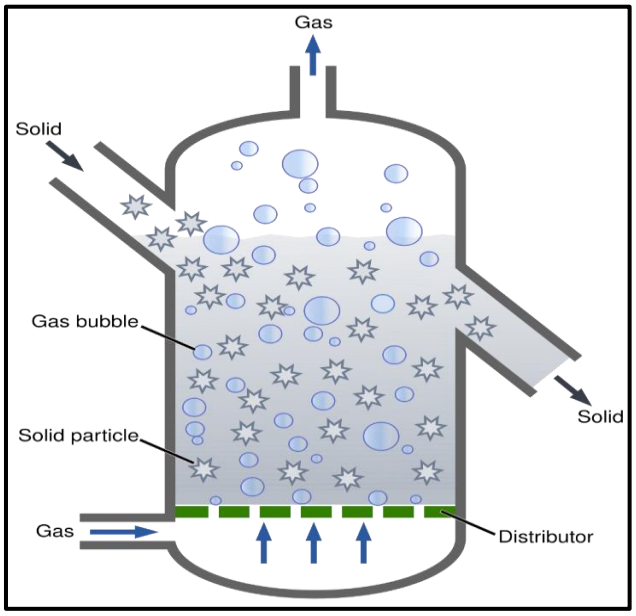


Fig.3. Schematic diagram of fluidized bed reactor (Howard., 1989)

Fluidized bed reactor also offers flexible operating temperature and pressure for hydrogenation of benzene. The operating temperature ranges from 150^0C to 300^0C and minimizes the formation of side products while maximizing the selectivity of cyclohexane. On the other hand, pressure range for fluidized bed reactor ranges from 1 atm to 10 atm. Here, higher pressure increases the reaction rate and enhance solubility of hydrogen to achieve the higher conversion of benzene to cyclohexane.

Different types of reactions can be carried out in fluidized bed reactor such as, catalytic cracking in petroleum industry, combustion and gasification of solid fuels (biomass, coal, waste material), oxidation and hydrogenation reaction. However, the selection of operating conditions depends upon the safety and equipment capabilities. Certain reactions may lead to plugging or fouling inside the reactor bed, which requires frequent cleaning and maintenance. Further, elutriation of fine catalyst particles can occur in fluidized bed reactor and creates problem for separation process.

1.3.3. Slurry reactor

Slurry reactors can be selected as an alternative for hydrogenation of benzene. Slurry reactors also offer an advantageous mass transfer along with catalyst utilization during hydrogenation reaction. In this type of reactor, catalysts were suspended in a reaction mixture, creating a slurry. Good mixing between reactants and catalyst can be observed, which helps to enhance the reaction rate. In slurry reactor catalyst is finely dispersed promotes a good contact with the reactant molecules.

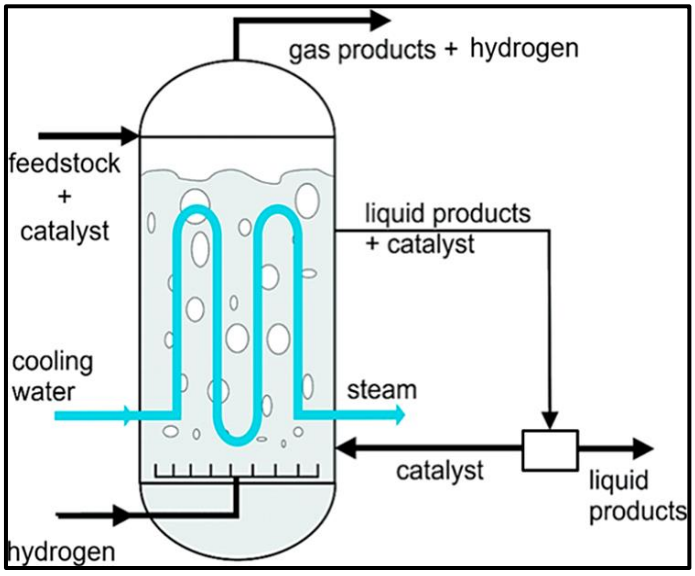


Fig.4. Typical slurry-phase hydrocracker (AI-Attas et al., 2019)

The suspension mainly ensures the contact between reactant and catalyst particles, results the increases in reaction kinetics and mass transfer. Catalyst particles can be easily separated from the reaction mixture in order to obtain an efficient catalyst recovery and recycling. The aforementioned approach is beneficial to facilitate cost savings and also minimizes waste generation compared to fixed bed reactor. However, slurry reactor also faces some of the disadvantages such as, low mass transfer in liquid phase, attrition and settling of catalyst particles.

1.3.4. Batch reactor

Batch reactors are mainly considered for the study of laboratory scale or small-scale hydrogenation reaction. In this type of reactor, reactors are loaded inside the reactor vessel and then the hydrogenation reaction is allowed to process under suitable conditions. After the completion of the reaction, product is removed and cleaned for the next batch. Batch reactors are suitable for exploring different types of reaction conditions, but not suitable in case of continuous production.

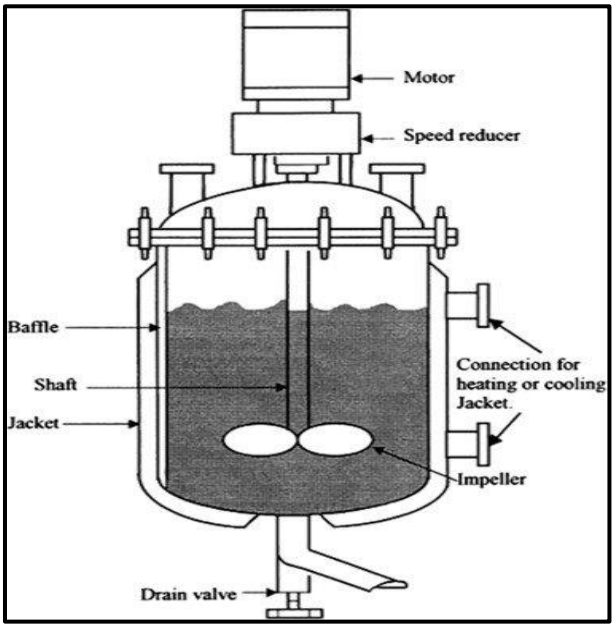


Fig.5. Schematic diagram of batch reactor (Ahmed., 2013)

Another limitation of batch reactor is the lack in use of resources. Here, reactants are typically fed in an excess amount to ensure a complete reaction within the reactor, but inefficient to utilize the reactant and lots of energy loss occur during the reaction. However, batch reactor also shows the limited control over reaction parameters such as temperature, pressure and mixing. In batch reactor, the reaction parameters are set at the beginning and remain constant throughout the reaction.

1.3.5. Membrane reactor

The reactor system consists of a membrane separator unit and allows an in-situ separation of reaction products, which leads the equilibrium limited hydrogenation reaction to completion. This type of reactor allows simultaneous hydrogenation and separation of reaction products. Membrane reactor is advantageous in case of improving the conversion rate, effectively utilize reactants and enhance selectivity. Similarly to other reactors membrane reactor contains catalyst that facilitates the hydrogenation reaction of benzene. It consists of a selective membrane that allows certain components to permeate while retaining the desired product.

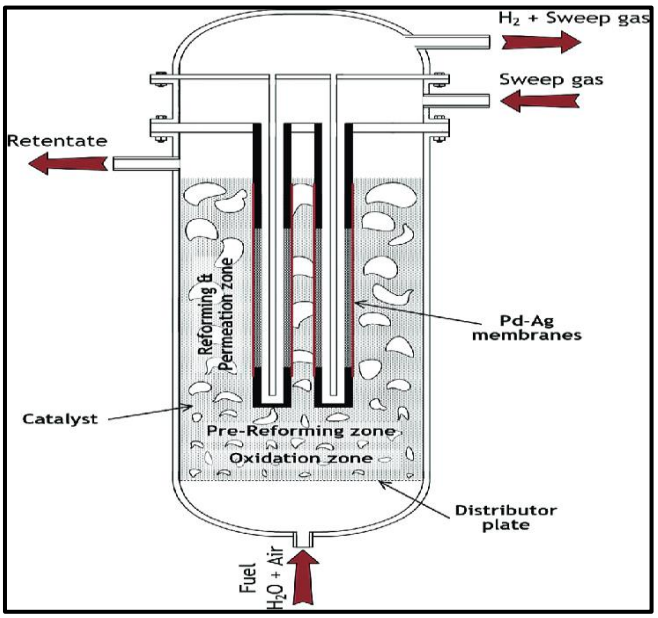


Fig.6. Schematic Diagram of membrane reactor (Marcoberardino et al., 2017)

Here, the H_2 gas diffuses through the membrane part of the reactor, creating a H_2 partial pressure difference which derives the completion of benzene hydrogenation reaction. Benzene molecules adsorb on the surface of the catalyst and react with H_2 molecules to produce cyclohexane. The presence of membrane helps to maintain a low partial pressure of H_2 which favours the forward reaction and enhance the benzene conversion rate.

1.4. Different types of catalyst synthesis methods

Catalyst synthesis prefers to the process of making catalyst. Catalyst plays a crucial role in order to speed up the chemical reactions, without undergoing any chemical change in itself. Catalysts are used in various industries, including petrochemicals, pharmaceuticals and environmental remediation. The synthesis of catalyst involves several steps such as selection of material, which represents the beginning step of catalyst synthesis process. Here, suitable materials like metal oxide, metals, organic compounds or zeolite are selected and the choices depends upon the specific reaction being catalysed. After the selection of material, preparation steps come into role which involves various techniques such as impregnation, precipitation, sol-gel and ion exchange. Each of the method leads to the deposition of catalytic species on the surface of a support material, by creating a structure that exposes the active sites. After preparation step catalyst are required to enhance their activity. So, calcination (heating in the presence of O_2), reduction (with the help of H_2 gas) process is used for the activation of catalyst and also to remove impurities. Brief descriptions about various types of synthesis methods are discussed.

1.4.1. Precipitation process

Precipitation process is a common method used for the catalyst synthesis with specific properties. The process involves with the formation of solid particles form a homogeneous solution through the addition of a precipitating agent. The process starts with the selection of precursor compound that will form the catalyst active sites and it must be soluble in the solvent. Precursor material is then dissolved in a suitable solvent or solvent mixture. Common types of solvents are ethanol, acetone, water or a mixture of water and organic solvents.

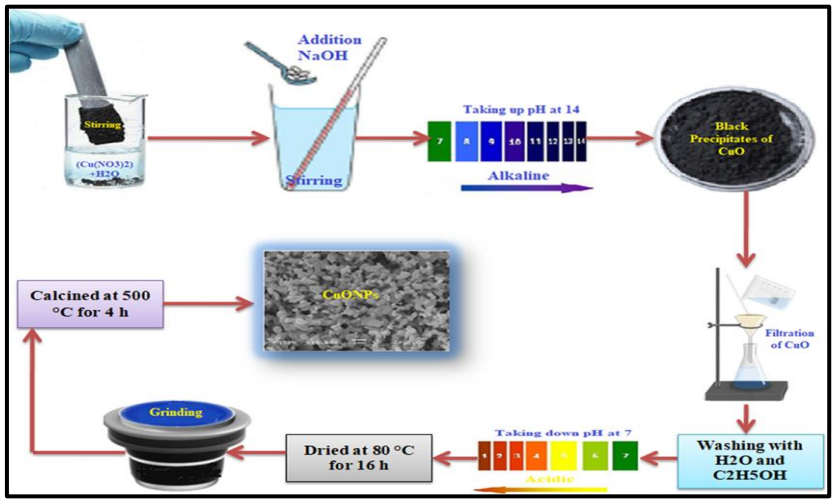


Fig.7. Schematic diagram of precipitation method (Haider et al., 2023)

Then a precipitating agent is added to the solution, causing them to from an insoluble solid particle (precipitate) by interacts with the precursor ions present in the solution. Common types of precipitating agents are salts, acids, bases or complex agents. In order to ensure the desired particle size, crystallinity and morphology, the reaction is carried out under a controlled condition of pH, temperature and mixing. After the completion of precipitation reaction, the solid precipitates are separated out by centrifugation or filtration and washed precipitates then dried to remove remaining solvents, which is then subjected to calcination at final stage.

1.4.2. Sol-gel Method

Sol-gel method is a versatile and widely used method for catalyst synthesis. The process involves the formation of colloidal suspension known as sol, which undergoes gelation to form a gel (solid type network), contains the desired catalyst species. In sol-gel method, a precursor solution is made at first, also known as sol and the solution typically contains metal salts, metal alkoxides. The solvents include isopropanol, ethanol or water. After the

preparation of precursor solution, hydrolysis is initiated with the addition of hydrolysing agent such as acid or water to the solution.

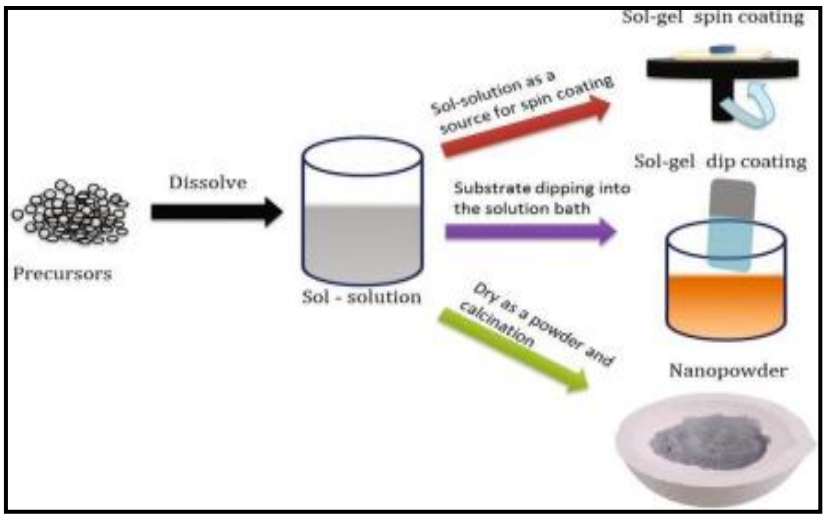


Fig.8. Methodology of sol-gel synthesis for metal oxide nanostructure (Thiagarajan et al., 2017)

Here, hydrolysis conducts cleavage of metal oxide bonds in the precursor molecules, which leads to the formation of metal hydroxides. After the hydrolysis reaction, the solution undergoes polymerization or condensation reaction. In polymerization reaction longer chains or networks formation occur and form chemical bonds like Si-O-Si in silica gel between the hydrolysed metal species. As condensation reaction progress, phase transition of the solution from liquid sol to solid gel takes place and form a 3-D network structure species that immobilizes the solvent within the gel matrix. At last, wet gel is dried to remove the excess solvent and then subjected to calcination, which promotes crystallization of the metal oxides. In sol-gel method, to control certain parameters such as, pH, gelation time and temperature become challenging in order to obtain a desired final product.

1.4.3. Electrodeposition Method

Electrodeposition or electroplating is a technique used ofr catalyst synthesis by depositing metal ions from an electrolyte solution on the surface of a conductive substrate (electrode). Electrodeposition method allows precise control over the morphology, composition and thickness of the deposited catalyst layer. In electrodeposition method, a suitable conductive substrate is selected onto which the catalyst will be deposited. Common substrate materials are stainless steel, titanium or carbon-based materials (carbon fibre, glassy carbon).

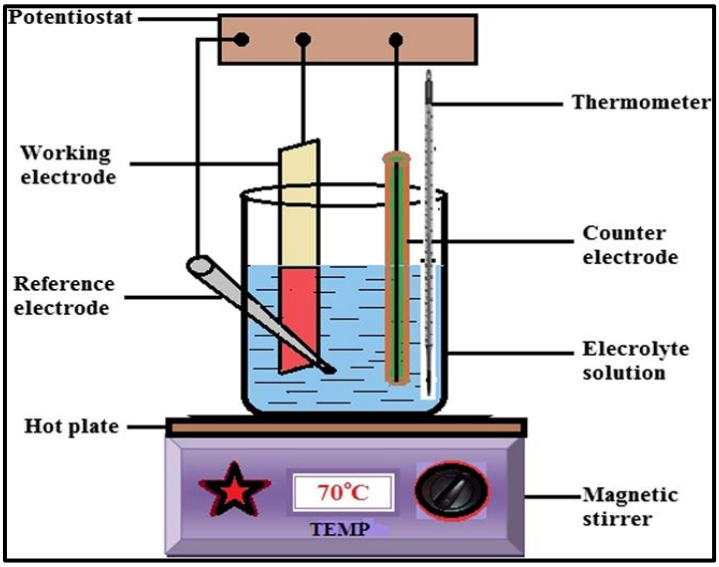


Fig.9. Effect of potential voltage on functional properties of AZO thin films, prepared by electrodeposition method (Kumar et al., 2018)

After that an electrolyte solution is prepared based on the on targeted catalyst, which may contain additives such as surfactants, complexing agents or buffering agents in order to enhance the properties of deposited catalyst. The conductive substrate acts as a working electrode within the electrochemical cell and it also contains reference and counter electrodes to fulfil the electrical circuit. Electrodes are placed inside the electrolyte solution and sealed to prevent contamination as well as evaporation during electrodeposition process. Then, potential difference is applied between the two electrodes (working and counter electrodes),

which drives the metal ions towards working electrode and this results the formation of thin layer on the surface of working electrode (substrate). The process continues until the desired thickness of metal catalyst is achieved.

1.4.4. Atomic Layer Deposition (ALD) Method

Atomic Layer Deposition is a sophisticated thin film deposition technique. This method is used for precise control composition and film thickness at the atomic scale. ALD found application in semiconductor manufacturing, in thin film technology. ALD contain a reaction chamber where precursor gases are sent and the deposition of catalyst occurs on the surface of the substrate inside the chamber. Reaction chamber is kept at a higher temperature to promote effective adsorption and reaction on the substrate surface. The precursor gases are mainly organometallic compounds or metal containing compounds.

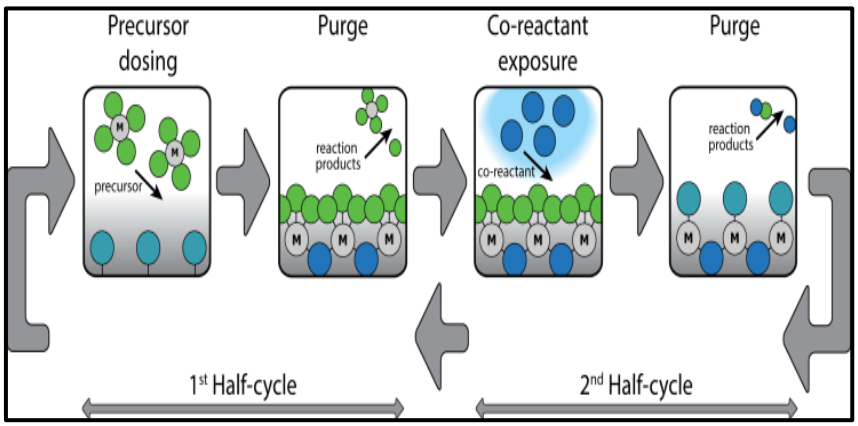


Fig.10. Development of atomic layer deposition (ALD) process (Vos., 2019)

The operation takes place in a cyclic way and in each cycle precursor gases are subjected sequentially inside the chamber. Whenever, the first precursor gas reacts with the substrate surface forms a monolayer through a surface limited reaction. After the completion of the reaction, inert gas is purged within the chamber to remove by-products and unreacted precursor component. On the next cycle of ALD, the reaction chamber is exposed to a second

precursor gas, which form the catalyst material by reacts with the chemisorbed species from the first step.

1.4.5. Impregnation Method

Impregnation method is a commonly used technique for catalyst synthesis. Active catalyst species are dispersed on the surface of a porous support material. The method mainly involves wetting of a support material with the help of a solution containing metal precursor to obtain an effective catalyst. Generally, support materials such as silica (SiO_2), aluminium oxide (Al_2O_3), titania (TiO_2), carbon nanotubes are considered. The precursor material is dissolved in a suitable solvent forming a precursor solution and then the support material is immersed within the precursor solution.

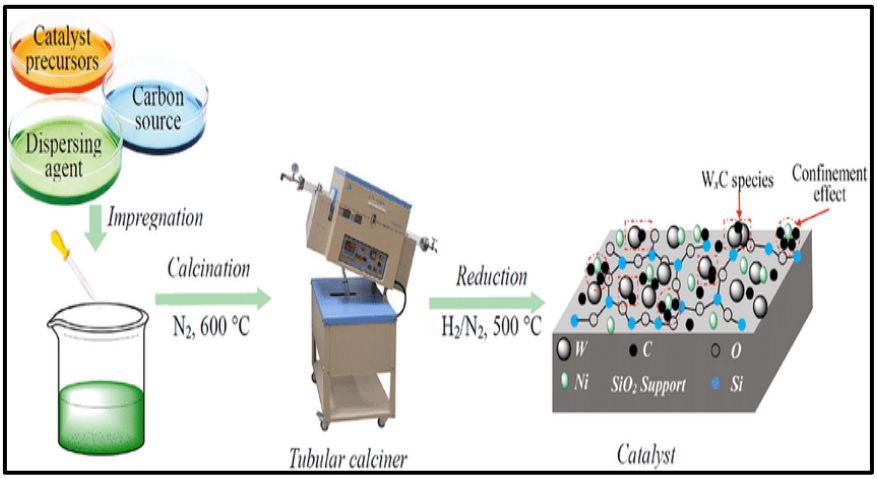


Fig.11. Preparation of Ni-W/SiO_2 catalyst by impregnation method (Xiao et al., 2018)

Due to the presence of porous structure in the support material, the solution penetrates into the pores and ensuring a uniform distribution of precursor material throughout the support matrix. Now, the whole excess solution is mixed for longer time duration with the help of a magnetic stirrer, which leads to a well dispersion of metal particles in order to achieve a desired structure of the catalyst. Here, the impregnation method can be carried out in various

way such as, dipping, incipient wetness impregnation, soaking or vacuum impregnation. After that, the excess solvent is typically evaporated with the help of drying process by applying gentle heat.

1.4.6. Chemical vapor deposition method

Chemical Vapor Deposition (CVD) is a widely used method for catalyst synthesis. In this type of technique deposition of a thin film of material occurs over the substrate through chemical reaction in vapour phase. CVD method is used in various sectors such as optics, catalysis, coatings and in semiconductor manufacturing. In CVD, precursor gases are introduced inside the reaction chamber with the help of a mass flow controller in order to maintain desired stoichiometry.

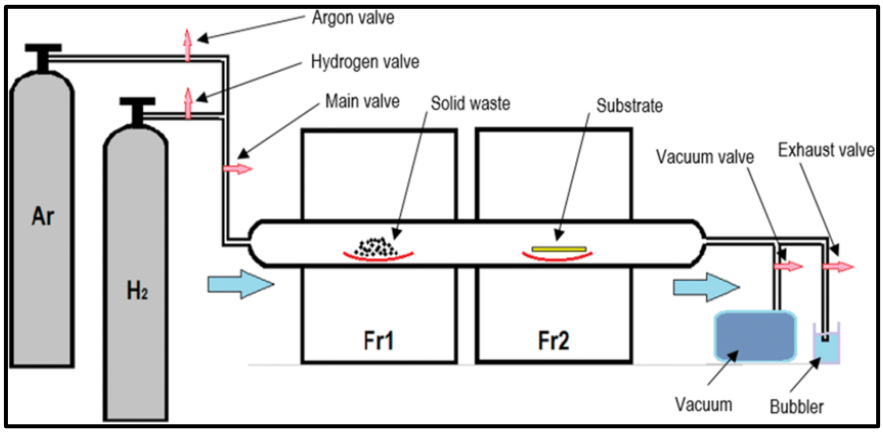


Fig.12. Schematic diagram for chemical vapour deposition method (Tahir et al., 2020)

Inside the reaction chamber precursor gases comes in contact with the substrate compound through diffusion or through carrier gas (H_2 or N_2 gas). Due to this contact between precursor gas and substrate, reaction takes place and the reaction. The interaction can involve pyrolysis, decomposition, reduction or oxidation of the precursor molecules transform into solid film. At initial stage, deposited material forms clusters or small nuclei on the substrate surface,

known as nucleation process. As more precursor molecules deposited on the surface of substrate, these clusters then grow into a continuous thin film. Various parameters are controlled during CVD technique to obtain a desired thin film property, where the parameters are precursor flow rate, pressure, temperature and deposition time.

1.5. Advantages of Excess Solution Impregnation Method (ESI)

The excess solution impregnation method offers several advantages compared to other methods for catalyst synthesis. ESI method is one of the widely used technique both in industrial and research field. Some of the key advantages are simplicity process, cost-effective, no impurities formation from starting to end and, higher loading of active metals on the support material is possible.

Other advantages of ESI method indicate the applicability for large scale production of catalyst, wide compatibility in case of the selection of support material, uniform dispersion of metal particles over the surface of support materials, high surface area of catalyst particles is obtained from ESI method due to the porous nature of support material. Properties of the catalyst can be customised with the help of ESI method, depending upon the parameters such as impregnation temperature, precursor concentration and activation condition.

1.6. Different types of catalyst and support materials

Support material in the context of catalyst, define as a matrix or substrate onto which catalytically active compounds are anchored or dispersed. Support materials play an important role in catalysts and provide a higher surface area for catalytic reaction. The high surface area increases efficiency of the catalyst by maximizing the contact between active sites and reactants. A support material also provides mechanical stability as well as enhances

the catalyst dispersion to achieve an effective reaction rate. However, support materials can vary widely based on their structure, composition, properties. The choices of support material is vital in case of catalyst design, as it can directly impacts the selectivity, activity, stability and overall performance of the catalyst in given reaction. Common types of support materials are oxides (TiO_2, Al_2O_3, SiO_2), zeolites, carbon-based materials and perovskites. Also based on the requirements such as to obtain higher surface area, increasing the active sites, lowering the activation energy and for ion exchange reactions, mono, bi or tri- metallic catalyst are considered as well.

1.6.1. Single support catalyst

A single support material catalyst also known as, mono-support catalyst. Only one type of support material is used to disperse or anchor catalytic active species. These types of catalysts consist of ions, metal nanoparticles or complex compounds deposited on the surface of a single support material. Higher surface area, mechanical stability and dispersion of the active phases can be observed within mono-support catalyst.

Selection of single support material depends upon various factors like, properties, catalytic application and compatibility with active phase. Furthermore, several reasons are involved with support materials such as, providing mechanical support sysstem, must be compatible with different types of metal species and must be cost-effective. Common types of single support materials include-

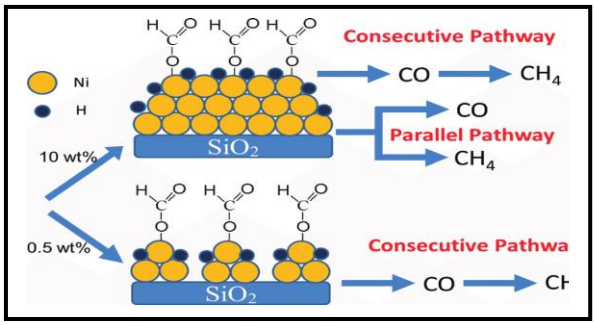
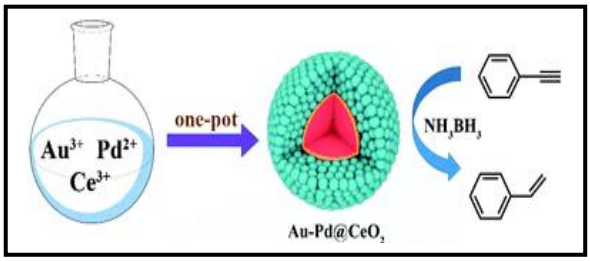
Table.2. List of some metal oxide support materials and their applications

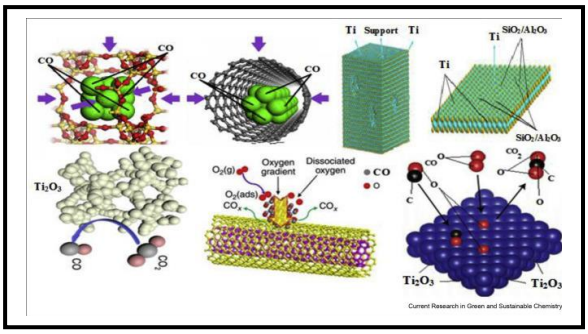
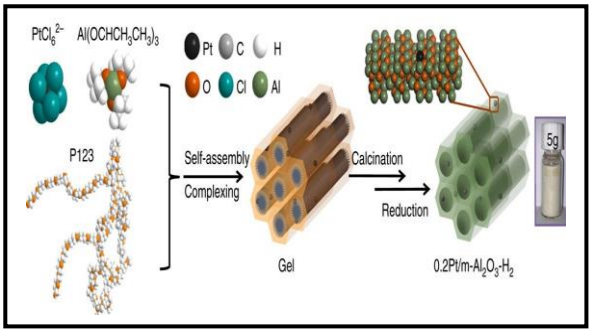
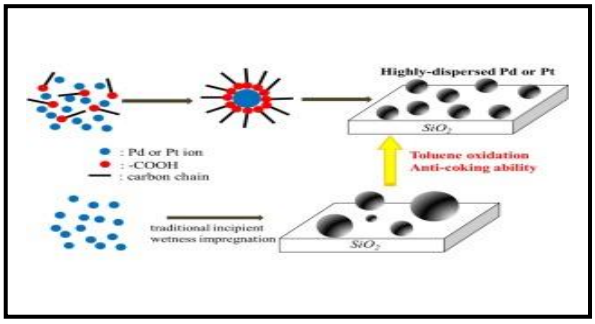
Alumina (Al_2O_3)	Widely considered for mechanical strength, high surface area, thermal stability. Alumina as a single support material is employed in various processes such as, dehydrogenation, hydrogenation and reforming reaction.
Titania (TiO_2)	Valuable for its stability, photocatalytic properties and in surface redox chemistry. TiO_2 as a single support material used environmental remediation, photocatalysis and solar energy conversion reactions.
Ceria (CeO_2)	Ceria is well known for its redox activity, catalytic versatility and oxygen storage. Applied in oxidation reactions, automotive catalysis and as a three-way catalyst (to coverts three pollutants, hydrocarbons (HC), nitrogen oxides (NO_x), carbon monoxide (CO)).
Silica (SiO_2)	Silica is chemically inert and has high surface area. In catalytic application, SiO2 as a support material requires neutral or acidic environments such as, oxidation and dehydration reactions.
Zirconia (ZrO_2)	Recommended for oxygen mobility, temperature stability and surface acidity. ZrO2 as a support material is applicable in oxygen storage, acid catalysed reaction and redox reaction.

1.6.2. Bi-metallic catalyst

Bi-metallic catalyst mainly consists of two different types of metal species (acts as the active sites) over a support material. Bimetallic catalyst exhibited synergistic effects due to the interactions between two metal species. These interactions enhance selectivity, catalytic activity and stability as compared to monometallic catalysts. Each metal species in bimetallic catalyst can be utilized for different purposes like; one metal species can offer active sites, while the other metal acts as a promoter or modifier. Furthermore, the dispersion, stability as well as activity of bimetallic catalyst can be increased by adding a high surface area support material. Various types of bimetallic catalysts are presents on the basis of their applicability, some of them are discussed below.

Table.3. List of bimetallic catalyst with different types of support

Ni-Co/SiO_2  (Wu et al., 2015)	Resistive towards sintering and carbon deposition compared to monometallic Ni catalyst. Helps to increase the longevity and stability in reforming reaction. Applied in steam reforming of methane for hydrogen production.
Au-Pd/CeO_2  (Liu et al., 2019)	This type of catalyst shows a higher activity of Pd with unique selectivity properties of Au and enables efficient oxidation of alcohols under controlled reaction conditions.

Co-Mo/TiO_2  (Dey and Mehta., 2020)	Used in petroleum refining for hydrodenitrogenation (HDN) and hydrodesulfurization (HDS) reaction to remove nitrogen and sulphur. One of the applications is the oxidation of alcohols to ketones and aldehydes in fine chemical synthesis.
Pt-Ru/Al_2O_3  (Zhang et al., 2017)	Applied in hydrogenation reaction to convert aromatic rings into cyclohexane, alkenes to alkanes. Also applied in direct methanol fuel cells (DMFCs) to generate electricity from electrochemical oxidation reaction.
Pt-Pd/SiO_2-Al_2O_3  (Wang et al., 2017)	Exhibits higher thermal stability and catalytic activity, which leads to an efficient conversion of pollutants in exhaust gases. Mainly used in catalytic converters for the oxidation of hydrocarbons, nitrogen oxides and carbon monoxides.

Some bi-metallic catalysts also resistive towards poisoning such as Ni-Mo catalyst resistive in sulphur poisoning, Cu-Zn catalyst is resistive poisoning by carbon monoxide (CO) gas in water-gas shift reaction.

1.6.3. Tri-metallic catalyst

As the name suggest, a tri-metallic catalyst is consisting of three different types of metal components, work together synergistically to catalyse of a reaction. Due to the presence of three metallic combination, enhances stability, selectivity and activity of the catalyst compared to bimetallic and monometallic. Tri-metallic catalysts are applied in various fields including, oxidation, hydrogenation, to convert hydrocarbons.

Different types of support materials are considered in order to increases their catalytic activity. Some of the common support materials are zeolite and oxide based such as alumina, silica and their applications are given below.

Table.4. Description of some tri-metallic catalysts

Pt-Pd-Rh supported on SiO_2	Compositions are Platinum, palladium and rhodium which supported on silica. Applied in automotive catalytic converters for the purification of exhaust gases (CO, NO_x, HC). Here, SiO_2 support provides thermal stability and also helps to prevent the aggregation of Pt, Pd, Rh.
Ni-Co-Mo supported on Al_2O_3	Consist of nickel, cobalt and molybdenum supported on alumina. The Al_2O_3 support provides high surface area and structural stability in order to obtain a desired dispersion of

Ni-Co-Mo supported on Al_2O_3	metal species. One of the usages is in hydrodesulfurisation (HDS) of petroleum feedstock for the removal of sulphur impurities.
Fe-Ni-Cu supported on zeolite	Greatly utilized in Fischer-Tropsch synthesis, to convert synthesis gas (CO, H_2) into hydrocarbons. In this type of catalyst, zeolite support controls the size, shape selectivity and distribution of synthesized HC. On the other hand, tri-metallic combination increases the selectivity and catalytic activity.
Pd-Au-Ag supported on SiO_2-zeolite	Consists of palladium, gold, silver supported on silica and zeolite combination. This type of catalyst can be used for partial hydrogenation of alkynes to alkenes. Here, SiO_2-zeolite combine support exhibits thermal stability, control the reactant and product diffusion in a hydrogenation reaction.

1.6.4. Carbon based support materials

Carbon based support material in catalysis plays a key role due to their high surface, unique properties and excellent thermal stability. Carbon base material provides a stable platform for anchoring metal species (active) and represents several advantages in catalytic application. Some descriptions of various types of carbon-based support materials are discussed below.

1.6.4.1. Activated carbon

Widely used in catalysis for providing higher surface area to volume ratio, ease of functionalization and chemical inertness. AC pertain a highly porous from of structure, characterized by a network of mesopores and micropores. This porous structure of AC gives

active sites for the deposition of metal species (catalytic elements), which leads to increase the catalytic activity. AC base material is mainly applied in gas phase reaction, adsorption reaction and for waste water treatment.

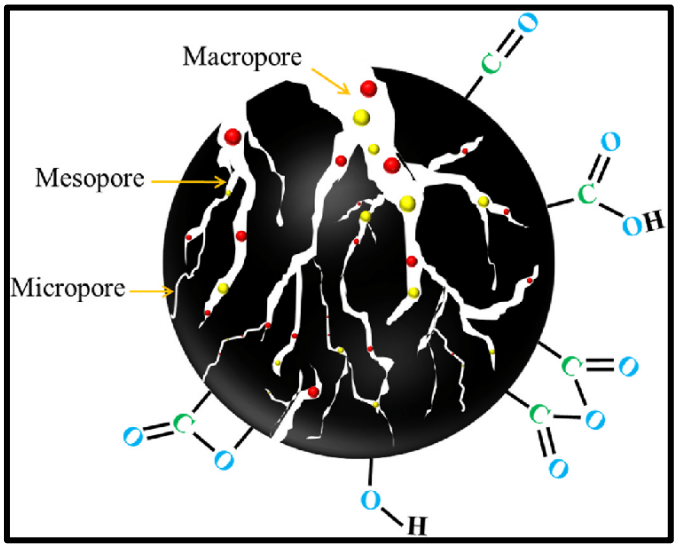


Fig.13. Pore structure and surface functional groups of activated carbon (Sultana et al., 2022)

The surface of activated carbon consists of various functional groups such as, carboxyl, hydroxyl, and carbonyl which adsorbs reactants in a catalytic reaction and facilitate their conversion into desired products. Further, activated carbon material has a high adsorption capability, that leads to enhance the adsorption-desorption cycles in reaction rates and selectivity.

1.6.4.2. Carbon nanotubes (CNT)

Carbon nanotubes exhibits excellent conductivity, and give higher surface area, which makes a suitable support for catalytic nanoparticles. CNTs are basically a cylindrical shape nanostructure material composed of graphene sheets and shows extraordinary thermal, mechanical and electrical properties. The 1-D structure of carbon nanotubes facilitates an

effective dispersion for metal particles. CNTs are applied in oxidation reaction, hydrogenation reaction and in electrocatalysis. Carbon nanotubes also shows an excellent electrical conduction due to their 1-D structure, where electrons can travel along the length of the tube with minimal scattering. For this reason, carbon nanotubes are highly applicable in nanotechnology and electronics field.

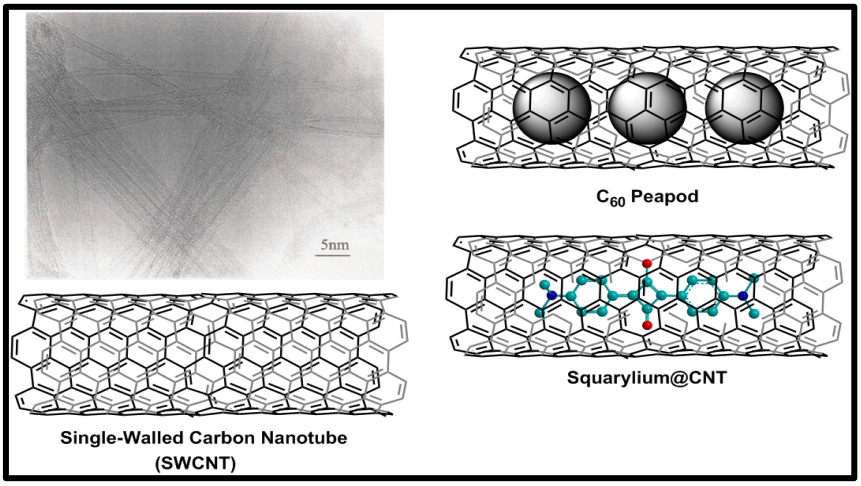


Fig.14. Breakup structures of Carbon Nanotubes (CNTs)

CNTs are good in case thermal conductivity and make it suitable as a reinforcing agent in composite material and for heat dissipation in electronics. Carbon nanotubes can be functionalized chemically by attaching various molecules in order to transform their properties. This type of customization for carbon nanotubes can be used in various fields such as, as a catalyst support, sensors or in biomedical devices.

1.6.4.3. Graphene

Graphene is a single layer of carbon atoms, arranged in a 2-D honeycomb lattice. The structure of graphene is characterized by sp^2 hybridized C-atoms, which is basically arranged in a hexagonal lattice. Further, delocalized electrons and π-electrons system presents in

graphene helps to enhance electrical conductivity. So, graphene can offer charge transfer process during a catalytic reaction which will leads to influence the reaction kinetics. This type of carbon-based material shows an excellent thermal, mechanical and electrical property makes it an efficient conductor of both electricity and heat. Graphene represents a basic building block for other carbon allotropes such as, carbon nanotubes, graphite and fullerenes.

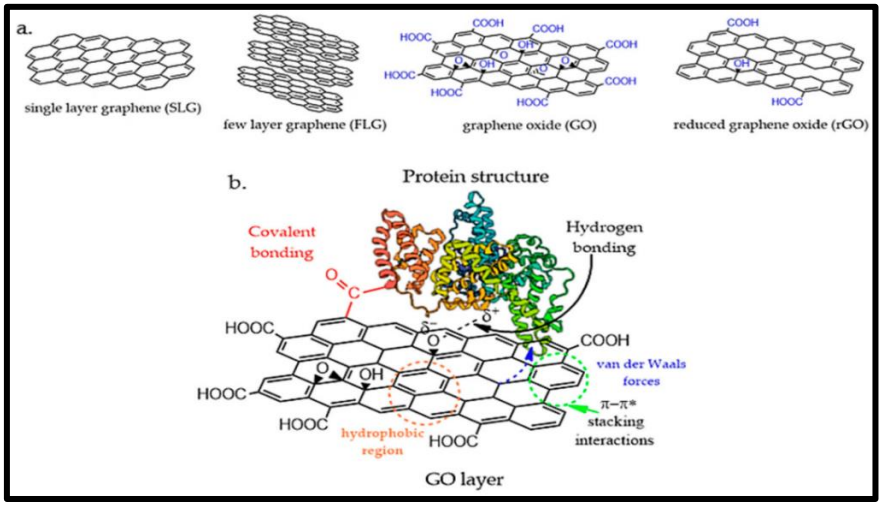


Fig.15. a) Structures of graphene nanomaterials and b) Illustration of possible covalent/non-covalent interactions between protein and GO structures (Biru et al., 2022).

Graphene also shows a tunable property in case of mechanical flexibility and chemical reactivity. Mainly, heteroatoms like, boron, N_2 are doped to optimize its performance as a catalyst for a particular reaction. Graphene allows 96% of light to pass through, which makes it a suitable material for conductive coatings. Other application of graphene includes in energy storage, electronics and as a sensor.

CHAPTER 2

LITERATURE REVIEW

CHAPTER 2

LITERATURE REVIEW

Si et al. (2023), worked on the hydrogenation of benzene by synthesizing Linde A-Type zeolite catalyst. LTA zeolite was synthesized from ball clay with two steps of calcination and with addition of NAOH/$Al(OH)_3$ (mass ratio 1:1.2/0.43) at temperature 600^0C. After that, hydrothermal treatment was carried out at 60^0C temperature for 48 hr introducing 3 wt.% of Ru^{+3}. The obtained zeolite with LTA structure was studied based on the hydrogenation of benzene at 150^0C, hydrogen pressure=5.0 MPa where 4000 mol/(mol.h) of turnover frequency was obtained for cyclohexane. The stability of the catalyst was demonstrated based on the higher conversion of benzene from 94.0% to 98.0% by using several cycling runs. Peyrovi et al. (2018), demonstrated the reduction of benzene in a mixture of toluene and benzene followed by hydrogenation reaction. The study mainly focuses on the development of different types of catalyst supports such as Ni/HZSM-5, Ni/HMS, Ni/HZSM5-HMS, Ni/Al_2O_3 and Ni/SiO_2. Kinetic of the reaction was studied at various hydrogen and benzene pressure along with two models "Langmuir-Hinshelwood", "Power Law". Both of the models allow good fit towards the experimental data and help to determine the kinetic parameters. The study further shows that Ni/Al_2O_3 provides the maximum conversion of benzene (99.19%) at 130^0C in benzene hydrogenation reaction whereas Ni/SiO_2 gives the maximum benzene selectivity (75.26%) at 130^0C as compare to other catalysts. Furthermore, kinetic evaluations and catalytic performances (activity, stability and selectivity) shown that Ni/SiO_2 is an effective catalyst for benzene hydrogenation reaction. Although, surface property like pore size is an important parameter as compare to other factors such as metal dispersion and acidity for this process. Tang et al. (2022), investigated the catalytic performance of Pd/CeO_2 catalyst via benzene hydrogenation reaction at temperature ranges from 100-200^0C under

atmospheric pressure. Impregnation method was used for the synthesis of Pd/CeO_2 catalyst by varying metallic Pd loading. The study shows that catalytic performance of Pd/CeO_2 depend upon the loading amount of metallic Pd. Increasing Pd loading from 1-3 wt.% results the enhancement of amounts of active Pd and adsorbed-desorbed of hydrogen on Pd/CeO_2 catalyst. On the other hand, on 3.5 wt.% of Pd loading reduces the amount of active Pd and adsorbed-desorbed of hydrogen on the catalyst surface. Ren et al. (2013), synthesized high-surface-area mesoporous $Ce_{1-x}Mn_xO_2$ mixed oxides through a surfactant-assisted assembly method, yielding nano-scaled particles with a fluorite structure and uniform mesoporous distribution. The authors reported that catalysts demonstrated exceptional catalytic activity in the total oxidation of propane, as evaluated using a micro reactor GC system. The authors investigated the influence of CuO as a promoter which revealed enhanced catalytic activity upon its addition, underscoring its potential to improve propane conversion. The authors also reported that catalytic performance was found to be influenced by the Ce/Mn ratio, surface area, and meso-porosity of the catalysts and catalyst with a Ce/Mn ratio of 1.5 exhibited the highest activity, suggesting its viability as a substitute for noble metal catalysts in propane total oxidation processes. Mohammadiana et al. (2019), work was based on the investigation of benzene hydrogenation in the BTX mixture using various carbonaceous catalysts. Furthermore, the work was also carried out at different temperature (130-190^{0}C), hydrogen pressure (2.3-5.2 Pa) and benzene concentration (2-8 vol.%). Under the mentioned conditions Ni-Graphene shows the best catalytic activity with over 94% conversion at 190^{0}C whereas Ni-activated carbon gives the highest selectivity of Cyclohexane (more than 60%) at 170^{0}C. Two kinetic models such as Power Law and Langmuir-Hinshelwood had been tested which provide a good fit based on the experimental data. Yang et al. (2008), investigated the catalytic combustion of benzene using metal oxides supported on SBA-15. The researchers synthesized catalysts via the incipient wetness method and characterized them using various

techniques including XRD, BET, TEM, ESR, and TPR. The authors reported that CuO/SBA-15 catalysts exhibited reduced surface area and pore volume compared to calcined siliceous SBA-15, indicating successful CuO incorporation. The authors also reported that CuO supported on SBA-15 showed the highest activity for benzene oxidation, surpassing CuO supported on MCM-41, and ESR results suggested that CuO dispersed on SBA-15 acted as the active site for benzene oxidation, with catalytic activity increasing with higher CuO loading. Li et al. (2018), uses CeO_2 nano cubes and nanorods as a support material to Pd/CeO_2 catalyst of 3wt%, prepared by hydrothermal method. The prepared catalyst (Pd/CeO_2) was then applied to investigate the benzene catalytic hydrogenation reaction within the temperature range 100-200^{0}C under atmospheric pressure. Morphological dependency of catalytic performance was observed for Pd/CeO_2 catalyst indicating that Pd/CeO_2 nanorod catalyst is more effective in benzene catalytic hydrogenation reaction. In this process 96.4% of benzene conversion and 100% of selectivity was obtained at 200^{0}C. Liu et al. (2005), showed several systems of vanadium oxide and K-promoted vanadium oxide catalysts, supported on different carries with the variations of V contents and K contents by incipient-wetness impregnation method. The researchers investigated catalytic performances for diesel soot catalytic oxidation with temperature-programmed oxidation reaction (TPO). The researchers utilized spectroscopic techniques (FTIR and UV–vis DRS) to determine the structure of VO_x species for vanadium supported on γ-Al_2O_3, SiO_2, TiO_2, and ZrO_2. The authors performed various characterization techniques such as thermal analysis, including thermogravimetric (TG-DTA) analyses and temperature-programmed reduction (TPR) to determine the thermal behavior and redox properties of K-promoting vanadium oxide catalysts, respectively. The results showed that the structure of supported-vanadium catalysts depends on the support materials and also on the V loading. The researchers reported at high V loading, VO_x species exist predominantly as polyvanadate species and V_2O_5, and the

catalytic activities of the catalysts for soot oxidation are correlated to their redox properties and the mobility of surface atoms. The catalytic activity for soot oxidation orders as Ti>Zr>Si>Al, and the sequence for selectivity to CO_2 formation is Ti>Zr>Si∼Al for the catalysts over different supports. The researchers reported that on adding potassium into supported vanadium catalysts the catalytic activity of soot oxidation can be improved. Guanghua et al. (2017), shows the establishment of the methodology for the generation of pore networks having arbitrary shapes can be easily accomplished, given that the domains itself can be mathematically explained using sets of inequalities. The construction of the pore network skeletons is achieved by employing a stochastic network algorithm, mostly involved with the cutting of the skeletons into the desired shapes and sizes. The newly cut shapes can also be embedded into different methods for the purpose of transplantation. The obtaining of four archetypical two-dimensional shapes as well as four three-dimensional shapes can be easily achieved by this method. Simulation of various scenarios can be easily observed through these mechanisms. These scenarios can often result in the analysis of the inherent properties of catalysts, such as effectiveness, diffusive capabilities and others. The variations in the performance of the catalyst can be effectively analyzed, therefore, leading to the discovery of the most suitable catalyst required for the specific study. Wang et al. (2012), worked on ceria-modified V_2O_5–ZrO_2/WO_3–TiO_2 catalysts with varying Ce concentrations for their performance in the NH_3-SCR process, both pre- and post-hydrothermal aging. The researchers reported that on addition of Ce the low-temperature activity of fresh catalysts was boosted, though it led to noticeable deactivation after aging. The authors performed various characterization techniques including XRD, XPS, H_2-TPR, and DRIFTS that revealed that Ce enrichment and enhanced redox properties, along with more active adsorbed nitrates on CeO_2-modified catalysts and contributed to improved SCR performance. The authors reported that reactivation post-aging was attributed to CeO_2 sintering and segregation on the

catalyst surface, indicating poor hydrothermal stability of the Ce component. Interestingly, additional NO_2 compensation post-aging markedly enhanced low-temperature SCR activity, highlighting Ce's high NO_2 sensitivity. Furthermore, ceria-zirconia-containing catalysts demonstrated superior SCR performance, achieving high NO_x conversions (>95%) and N_2 selectivity (>98%) across a wide temperature range (200–500°C) in simulated exhaust conditions. Ding et al. (2021), reported a series of 70 wt.% Ni supported highly adaptable catalysts prepared by the co-precipitation process. The main aim is to reduce the cost of dehydrogenation/hydrogenation catalysts and improve the catalytic activity in order to achieve the commercial application of Liquid Organic Hydrogen Carriers (LOHCs) Technology. The catalysts were used in the hydrogenation process of several LOHCs compounds such as N-propyl carbazole, Benzene, dibenzyl toluene and N-ethyl carbazole. Adjusting Al, Si ratio for Ni70/AlSiO-1/1 catalyst molar ratio of 1:1 shows the highest activity of the catalyst for the hydrogenation of LOGCs. Furthermore, Ni70/AlSiO-1/1 catalyst was used for the hydrogenation of N-propylcarbazole using 5-cycles. Glotov et al. (2019), tells us about the modification of Ni/Al_2O_3 with phosphoromolybdicheteropolyacid (HPA) and chromium compound. Basically, bimetallic catalyst (BMC) was used for hydro-conversion of aromatic hydrocarbons (ArH) such as toluene, benzene, and hydro-methylation of pure toluene. Bimetallic catalyst (BMC) shows the highest activity as compared to two component (Ni-HPA, Ni-Cr) and conventional Ni/Al_2O_3 catalyst. The activity of bimetallic catalyst (BMC) for hydrogenation of toluene and benzene increases to 34-38 mol/kg.h whereas hydro-demethylation of toluene performed with improved benzene yield of 81% and selectivity 90.3%. Sulfur tolerance of bimetallic catalyst (BMC) was demonstrated by hydro-demethylation of toluene containing up to 500 ppm. Chen et al. (2019), demonstrated about the experimental and theoretical approaches of designing Ru base catalyst in order to enhance the yield of Cyclohexane from benzene using Benzene hydrogenation process. The process

itself is an economically interesting and technically challenging reaction. Kinetic study, basic thermodynamics, Ru-Zn system (including both inorganic additives and organic additives), Ru-M-B-based catalytic systems and Ru-M catalytic systems were discussed. No-additive Ru-BZSS catalyst was developed in order to get a deep understanding about its activity. The work also based on the solving challenges in current work and to open possible opportunities. Yao et al. (2014), investigates NO reduction by CO over model catalysts of $CuO/\gamma\text{-}Al_2O_3$, $Mn_2O_3/\gamma\text{-}Al_2O_3$, and $CuO\text{-}Mn_2O_3/\gamma\text{-}Al_2O_3$, both before and after CO pretreatment at 300 °C. The authors reported that the CO-pretreated $CuO\text{-}Mn_2O_3/\gamma\text{-}Al_2O_3$ catalyst demonstrated superior catalytic activity. The researchers employed various characterization techniques including XRD, XPS, UV/Vis diffuse reflectance spectroscopy (DRS), Raman, and H_2-temperature-programmed reduction (TPR), a proposed interaction model between dispersed copper and manganese oxide species on the $\gamma\text{-}Al_2O_3$ surface is presented. The study introduces a new concept, surface synergetic oxygen vacancy (SSOV), describing the oxygen vacancy formed between individual Mn and Cu ions in CO-pretreated $CuO\text{-}Mn_2O_3/\gamma\text{-}Al_2O_3$ catalysts. In addition, the role of SSOV is elucidated through NO temperature-programmed desorption (TPD) and in situ FTIR experiments, demonstrating its importance in NO reduction by CO. The study underscores the significant differences in SSOV properties compared to surface oxygen vacancies (SOVs) formed in CO-pretreated $CuO/\gamma\text{-}Al_2O_3$ and $Mn_2O_3/\gamma\text{-}Al_2O_3$ catalysts, highlighting the pivotal role of SSOVs in catalytic activity. Parsafarda et al. (2019), tested Ni catalyst supported on nano porous material for the vapor phase benzene hydrogenation reaction. The catalysts were prepared using Impregnation method and the study shows that Ni/Folded sheets Materials-No. 16 has the highest stability with lower deposition of coke (less than 1.1%) along with best selectivity of benzene (more than 84%). Kinetics of the process is considered as a function of hydrogen and benzene pressure at various temperatures. Power Law and Langmuir-Hinshelwood models were taken

to compare with the experimental data and also to determine kinetic parameters. Feng et al. (2023), depicted that during biomass conversion, solvent plays an important role determining reaction mechanism and product selectivity. In this case Ni/β_{40} was prepared followed by deposition-preposition method and used for catalytic hydro conversion (CHC) of benzyloxy benzene (BOB) into dicyclohexylmethane (DCHM) or toluene. Results show that atmosphere, solvent types and Ni_{20}/β_{40} are effective in product regulation. DCHM was produced with a selectivity of 94.6% under the respective conditions (180^0C, 2 MPa H_2 and 4hr) whereas phenol and toluene were obtained over optimal condition (180^0C, 0.5 MPa H_2 and 4hr). Conversion of BOB depends upon the cleavage of >CH-O- bond induced by the addition of H^+.

Li et al. (2006), investigated the complete catalytic oxidation of toluene using Cu−Mn doped catalysts with mesoporous and microporous structures, namely Cu−Mn/MCM-41, Cu−Mn/β-zeolite, Cu−Mn/ZSM-5 (with SiO_2/Al_2O_3 ratios of 25 or 38), and Cu−Mn/porous silica, in the presence of excess oxygen. The authors reported that mesoporous catalysts exhibited the highest catalytic activity, attributed to lower coke formation facilitated by their unique mesoporous structures. The researchers reported that the bimetallic Cu−Mn−MCM-41 supported catalyst displayed superior oxidation activity compared to single metal catalysts (Cu−MCM-41 and Mn−MCM-41), indicating the enhanced performance of highly dispersed Cu−Mn mixed oxides on mesoporous structures, likely providing active sites for complete toluene oxidation. Malins et al. (2023), depicted Screening test on various prepared and commercial metal catalysts includes Re, Pt, Pd, Ru, Rh, Ni and Au using solvent free hydrotreating of rapsid oil (RO) to produce renewable hydrocarbons (RH). Specifically supported Re, Ru, Rh (5%), Ni (65%) catalysts were the most active and gave RH yield upto 85% with a full conversion of RO in a shorter residence time (10 min), reaction condition (340^0C, 10 MPa H_2 pressure). SiO_2-Al_2O_3 supported Ru (5%) catalyst showed an effect on –

C-C- bond reactions, suitable for applications in RH synthesis. The catalyst performed similarly to active supported commercial noble metal catalysts in the HT process of RO and was reusable for up to three reaction cycles, although catalyst deactivation led to significant changes in the obtained hydrocarbon composition. Model compounds such as benzene, toluene, tetralin, guaiacol, and n-nonadecane were used to investigate catalytic effects. Overall, the study highlighted the potential of Ru_5SAp for renewable hydrocarbon production from different raw materials, including fats, oils, phenols, and fossil-based feedstocks. The study specifically details the synthesis of CdS and Ru-containing halloysite-based nano catalysts through modification with organic ligands and microwave-assisted wetness ion impregnation. These nano catalysts were then employed in the catalytic hydrogenation of benzene, its homologues, and phenol. The research optimized the core-shell architecture, metal particle size, and seeding density to achieve high reaction efficiency. The creation of Co-hallosite using ligands and azines is an important part of this work. Co-halloysite catalyst contained 16 wt.% of cobalt and possesses hydrogen evolution rate of about 3.0 L/min per gram of catalyst. The catalyst itself is based on a cost effective, natural clay nanomaterial (halloysite) offering an economically viable and safe option for industrial application. However, scalability of these catalysts confirms widespread usage in various industrial processes. Zhu et al. (2000), studied the effects of HCl, HNO_3, and HF treatments of carbon on N_2O and NO reduction using 20 wt.% Cu-loaded activated carbon. The authors reported that Cu_2O/AC–HNO_3 exhibits the highest activity for both N_2O and NO reduction, followed by Cu_2O/AC, Cu_2O/AC–HF, and Cu_2O/AC–HCl. This activity sequence correlates with the amount of CO_2 evolved during temperature-programmed desorption (TPD) experiments and catalyst dispersion. The researchers reported that N_2O shows a higher reaction rate and sensitivity to acid treatments compared to NO. Additionally, the presence of gas-phase O_2 has contrasting effects on N_2O and NO reduction. The study highlights the significant role of

carbon surface chemistry in rationalizing these findings and discusses their mechanistic and practical implications. Moreover, the effects of oxygen surface groups on the pore structure of supports and catalysts are analysed. Wang et al. (2018), suggested the impregnation method for the synthesis of ZrO_2-r-Al_2O_3 which is developed with lanthanum, indium and nickel species. Activity of the catalyst was studied on the basis of removal of benzene, sulfides in fluid catalytic cracking gasoline using a fixed bed reactor. Under the suitable conditions such as reaction temperature 423 K, metal loading 15%, reaction time 60 min, space velocity $3h^{-1}$, and reaction pressure 1MPa gives conversion of benzene to toluene and dimethylbutane reach 100%, 19.9%, 48.9% and 50.9%, respectively. On the other hand, octane number of the product increased by 2 units and sulfur content reaches zero. Furthermore, the catalyst was potentially involved in the hydrogenation process and takes almost 30 hr with no loss in activity. Mokrane et al. (2017), represents Ni nanoparticles supported on alumina used for benzene hydrogenation process, prepared by ethylene glycol reduction method. Obtained metal particles falls under the size range of 2-29 nm and its catalytic performance was determined by gas phase benzene hydrogenation. In this case the metal dispersion effect is found to be effective on the basis of metal loading. Study based on H_2-TPD showed that the hydrogen storage changes with varying the metal loading and furthermore, support material also takes part in case of hydrogen storage through H spillover. The catalytic activity of Ni/Al_2O_3 catalyst was dependent upon the particle size, metal loading and storage of hydrogen in the catalyst. NiEG-05 shows higher specific rate during the hydrogenation reaction of benzene compared to other catalyst and this attributed the presence of active sites of nickel catalyst on the support surface material. Molina, Poncelet. (2001), studied the activity of Ni/Al_2O_3 catalysts in the hydrogenation of benzene. The catalysts were prepared with nickel content ranging from 0.4-3 wt.% using Ni acetylacetonate as a precursor. Particle sizes, determined by hydrogen chemisorption, varied from 1.9 nm to 8

nm depending on nickel content and reduction temperature. Preliminary decomposition of organic ligands at 250°C followed by reduction enhanced activity compared to direct reduction. The authors reported that catalysts reduced at 350-400°C were more active than those reduced at higher temperatures. Catalysts with nickel content of 1 wt.% and 1.6 wt.% were most active. Turnover frequency dependency on particle size suggested structure sensitivity below 4 nm. Unreduced nickel fraction also influenced activity. $Ni(acac)_2$ was deemed a valuable precursor for preparing efficient and stable catalysts with low nickel content based on turnover frequency comparisons with literature values. Savva et al. (2008), shows different types of methods (Sol-gel, dry impregnation, co-precipitation) were used for the synthesis of nickel supported alumina catalyst and was evaluated by the hydrogenation of benzene present in gasoline. Evaluation was carried out by considering a high pressure and temperature fixed bed reactor in which a stream of surrogated reformate gasoline (consists of toluene, benzene and hexane) was sent to the reactor in gas-phase. The study shows that, sol-gel procedure is followed up by supercritical drying, produces promising catalyst for the hydrogenation reaction process. Basically, sol-gel procedure is more effective in case of Ni phase dispersion as well as interaction with the surface of support material. On the other hand, co-precipitation process exhibited important activities but much lower than sol-gel and things were also similar for dry impregnation in which case calcinations step reduces the catalyst activity. Peyrovi et al. (2018), had worked on the reduction of benzene in reformate gasoline using Ni supported on Al_2O_3, SiO_2-Al_2O_3 and SiO_2. The catalysts were prepared by sol-gel method in order to get effective dispersion of Ni and a strong interaction with support material. The investigation was carried out with the help of a continuous fixed bed micro reactor where reformate gasoline was considered as a feed. Operational temperature of the fixed bed reactor was around 398-473K and under atmospheric pressure. To understand the performance of the catalyst different space velocities, H_2/benzene molar ratios were

considered. Study showed that Ni/FDU-12, Ni/SiO_2-b and Ni/SiO_2 reduce the benzene concentration less than 1 vol.% at 423K. Ni/Mil-53(Al) and Ni/MSA represents the higher conversion for toluene compared to other catalysts and Ni/SiO_2 catalyst gives the highest conversion of benzene at 423K. Within the lower value of space velocity and H_2/benzene molar ratio, benzene molecules get a better chance to take participate in hydrogenation reaction. The study investigates the hydrogenation of benzene to cyclohexene over Ru/Al_2O_3 catalysts in the presence of water mainly focusing on the interplay of various factors such as reaction conditions, ruthenium precursors, and catalyst pretreatment. The reaction occurred under kinetic control and significant mass transfer limitations, indicating the complexity of the process. Although the presence of water complicates the straightforward attribution of cyclohexene formation to physical effects alone, it underscores the multifaceted nature of the reaction mechanism. Furthermore, while mass transfer limitations are crucial for achieving high selectivity at elevated conversion levels, they also underscore the importance of optimizing reaction conditions for efficient catalytic performance. The authors reported that catalyst pretreatment under hydrogen, without the presence of benzene, has shown to enhance selectivity towards cyclohexene, suggesting the significance of catalyst activation steps. In contrast, pretreatment under nitrogen did not elicit any discernible effect, underscoring the specificity of the hydrogen pretreatment. Moreover, catalysts derived from $RuCl_3$ demonstrated greater selectivity compared to those derived from chlorine-free precursors, indicating the influence of precursor chemistry on catalytic performance. Mohammadian et al. (2022), investigated about the factors affecting the specific rate of nickel supported catalysts. Wet-impregnation method was used for the synthesis of Ni (25%) supported on HMS, HZSM-5, HMS-HZSM-5, γ-Al_2O_3 and SiO_2. Hydrogenation of benzene was carried out within the temperature range of 130-190°C and under atmospheric pressure. Furthermore, main parameters such as flow of hydrogen, weight percentage of benzene and reaction

temperature were optimized using Response Surface Methodology. 8wt.% of benzene was considered to obtain the optimize values from Response Surface Methodology and the respective temperature was 130^0C, over Ni/Al_2O_3 catalyst. Jiang et al. (2019), reported about carbon composed Raney nickel catalyst with a cage-like structure reinforced in-situ carbon nanotubes and as a carbon precursor Phenol formaldehyde resin was selected for the preparation of this catalyst. Powder form of two compounds phenol formaldehyde resin, Ni-Al (48 wt.% Ni) alloy firstly mixed with each other, then the mixture was compressed, cured and carbonized, followed by alkaline leaching. The obtained carbon-composed possesses acceptable hydrogen adsorption capacity, higher stiffness and good catalytic property. Comparing with other commercial catalysts this carbon-composed Raney Nickel catalyst shows higher selectivity and similar type of catalytic activity. The use of carbon composing method to make Raney cobalt, Raney nickel, and Raney copper were very important fix-bed catalysts for chemical industry.

Pawelec et al. (2007), studied on modified silica-alumina supported nickel catalysts (Ni/ASA) by incorporating electron donor (Li) or electro acceptor (Pd) elements to investigate factors influencing catalyst thio-resistance in benzene hydrogenation. The catalysts were tested in benzene hydrogenation and the hydro-conversion of pyrolysis gasoline (PyGas), and compared with zeolite NaY-supported catalysts. The researchers employed various characterization techniques to analyze the catalysts. The monometallic Ni/ASA catalyst with 24 wt.% Ni showed the highest activity in both benzene hydrogenation (+S) and PyGas hydro conversion. The authors reported that catalyst characterization indicated that metal and acid site concentrations governed catalytic activity, with hydrogen adsorption ability being crucial. The researchers also reported that S-poisoning increased with catalyst reactivity but decreased when coke deposition inhibited S-compound adsorption. Pd promotion of nickel catalysts proved important for both hydrogenation and ring-opening

reactions in PyGas transformation. Shin et al. (2019), described about series tests on hydrocracking (HDC) and hydrotreating (HDT) of fluid catalytic cracking (FCC) to convert light cycle oil (LCO) into light aromatics consists of toluene, benzene, xylenes (BTX). In this process a fixed bed down flow reactor was used under the application of medium pressure (6 MPa). Two types of LCOs feed stocks LCO-1, LCO-2 (contain a small fraction of heavy tri+-aromatics and alkyl(C^{2+})-carbazoles) were used. Comparison between NiMo-S, NiW-S, CoMo-S on γ-Al_2O_3 support and LCO HDT a commercial catalyst shows that NiMo-S/γ-Al_2O_3 catalyst determines highest selectivity of di^{+}-aromatics with minimal loss of aromatics at high HDN conversion. Among the three catalyst Mo-S, Mo-S/BZ(10) and H-ZSM-5, Mo-S/BZ(10) gives the highest yield BTX in HDC model whereas Mo-S shows moderate power in HYD and H-ZSM-5 favor towards dealkylation of alkyl aromatics. Due to the limited conversion of C^{11+}, hydrotreated LCO-1 (HDT-LCO-1) over Mo-S/BZ(10) catalyst indicates lower yield of BTX-aromatics. Therefore, Mo-S/BZ(10) and NiMo-S/γ-Al_2O_3 were the most promising catalysts for the conversion of light cycle oils into BTX-rich light aromatics. Stanislaus and Cooper. (1994), highlighted the high levels of aromatic compounds in diesel fuel not only compromise its quality but also play a significant role in the formation of harmful emissions in vehicle exhaust. These emissions pose serious health risks, prompting regulatory bodies in both Europe and the United States to impose stricter limitations on the presence of aromatics in diesel fuels. The regulations aim to mitigate the adverse health effects associated with diesel exhaust and to reduce environmental pollution. The study tells that by reducing the aromatic content in diesel fuels, the goal is to improve air quality and public health while also promoting the development and adoption of cleaner, more sustainable transportation fuels. Meyer et al. (2021), suggested that calculations of micro kinetic modelling (MKM) and density functional theory are used to understand the binding energy of benzene which is responsible for catalyst cyclohexene selectivity. To correlate

elementary reaction on 3-fold active metal sites, scaling correlations and Brønsted−Evans−Polanyi (BEP) were used. Based on BEP correlations, thermo-chemical relationships, H_2 dissociation and binding energy of benzene were required in MKM for the prediction of benzene hydrogenation selectivity and activity. The study also shows that to gain an optimal balance over activity and selectivity for Cyclohexene formation intermediate binding energy of benzene plays an important role. Bayesian inference approach predicted uncertainties in the intercept of BEP and slope and scaling relationships which were propagated in MKM for the quantification of uncertainty in catalytic performance. Ni_3Ga and Ni_5Ga_3 were considered to be highly selective catalyst for benzene hydrogenation process. Yu et al. (2018), shows the effect of using coated Ru particles with a film of hydrophilic materials on benzene hydrogenation process. In this case, Sol-gel method was used for the preparation of Ru-XO_2 catalysts (X = Zr, Ti, Si). Basically, amorphous mesoporous materials such as ZrO_2, TiO_2 and SiO_2 were coated on Ru particles. During partial benzene hydrogenation process, Cyclohexane and benzene dissolved in the water phase onto the Ru particle which is then suppressed by the mesoporous coating film. After that diffusion of benzene is retarded by hydrogen bonding due to the presence of OH groups in hydrophilic materials. Ru-TiO_2 catalyst shows the highest conversion of benzene 85.0% along with maximum yield of 52.6%. Xue et al. (2017), reported the preparation of Ru/TiO_2 catalyst where the catalyst is encapsulated by TiO_2 coating (denoted Ru/TiO_2-p-TiO_2) and metal Ru particles serve as active sites for benzene hydrogenation reaction. Basically, benzene hydrogenation process is one of the most promising techniques to obtain Cyclohexane as well as intermediates for the production of value-added fine chemicals. The study also depicted that due to the shielding effect of TiO_2 layer, hydrogen molecule can easily diffuse into the Ru surface. DFT calculations and CHE-TPD shows that Cyclohexane has much activation energy and more beneficial in case of desorption for hydrogenation over TiO_2 surface. The

work also accounted large catalytic performance (selectivity of Cyclohexane 76.6%, conversion of benzene 98.1%) and yield of Cyclohexane. Girgis and Gates. (1991), provides a critical and comprehensive review of catalytic hydro processing reactions, focusing on the hydrogenation of aromatic hydrocarbons, hydrodesulfurization, hydrodenitrogenation, and hydrodeoxygenation. The study presents data on thermodynamics, reactivities, reaction networks, and kinetics, organized by reaction type. The researchers had addressed competitive reactions and inhibition effects in separate sections. The summarized results are deemed reliable and valuable for guiding process modelling in the hydro processing of heavy fossil fuels. Designed as a reference, the paper presents quantitative data in tables and figures, supplemented by a table of contents and a chart featuring the names and structures of organic compounds. Alimohammadi et al. (2021), represents selective benzene hydrogenation using a mixture of normal heptane (5 vol.% of benzene) and benzene over various kinds of catalyst. The study was further investigated by changing the support materials such as Pd/13X, Pd/Al_2O_3 and Pd/ZSM-5 and the modification was developed by considering specific amount of palladium nitrate in an aqueous solution. Catalyst assessment setup was conducted to evaluate the performance of the catalysts. The catalytic hydrogenation of benzene was carried out at optimized reaction conditions H_2/(feed hydrocarbon) = 1.3 (molar ratio), reaction temperature 200^0C, operating H_2 pressure 1MPa and the weight hourly space velocity (WHSV) = 25 hr^{-1}. Among the aforementioned catalyst Pd/13X gives the maximum benzene conversion (90%) and shows minimum light-cut production under the optimal condition. Furthermore, the declining activity of Pd/13X was higher as compared to other catalysts from 90% to 81% under the specified time duration of 20hr but, shows effective catalytic activity under the similar time duration on stream. Kordulis et al. (2001), investigated the desulfurization of fluid catalytic cracking (FCC) gasoline using NiW supported on γ-Al_2O_3 catalysts, prepared by two methods: conventional non-dry impregnation (NDI) and a new

technique called equilibrium deposition filtration (EDF), modified (MEDF) for practical catalyst preparation. The study has been divided into two parts: the first part represents the methodology and characterization results of catalyst preparation, in the second part, catalyst evaluation is described, comparing HDS, hydrogenation (HYG), and isomerization (ISO) activities with those of a commercial catalyst. The authors reported that the MEDF method showed promise over the NDI method for preparing NiW hydrotreatment catalysts. The NiW–MEDF catalyst exhibits higher HDS activity, comparable to a commercial CoMo catalyst, and superior HYG and ISO activities. The enhanced catalytic activity is attributed to the high dispersity of supported phases achieved by the MEDF preparation method. Ye et al. (2017), described about a method called stochastic network algorithm to generate pore networks on an arbitrary shape which can be mathematically described by inequalities. The pore network can be cut into a new one to generate a pore network cutting algorithm. Mainly, pore structure of four three dimensional shapes (hollow cylinders, trilobes, spheres and cylinders) and four two dimensional shapes (cross sections of wheels, trilobes, four-holed rings and spheres) are constructed in order to study reaction of catalyst Pd/c-alumina and also to simulate diffusion. The study shows that particle shape and randomness of the pore network affect the performance of catalyst. Method used in this work is ideal to study the effect of pore network and shape of the particle to understand the influence of porous particle in catalysis and other application. Rao et al. (2018), predicted that Ru based catalysts were promising towards benzene hydrogenation reaction. In this case, a novel core-shell catalysts were synthesized by introducing B-doped ZrO_2 on Ru/ZrO_2 particles (hydrogen dissociates on the inner surface of Ru) acts as an adsorption site for benzene. Ru/ZrO_2-BIJ5% catalyst demonstrated the optimal synergistic catalysis between medium/weal-strong Lewis acid site and metal Ru for which adsorption-desorption of benzene and Cyclohexen occur. Without using any additives almost 53.1% of benzene conversion and 58.8% of cyclohexane

selectivity were obtained. Sun et al. (2018), had used precipitation method to synthesize Ru-Zn catalyst and investigated the impact of sodium hydroxide (NAOH) modification on the selective hydrogenation of benzene to cyclohexene. Due to the addition of NaOH (from 0 to 0.6 molL^{-1}) (improved by ZnO dispersion) on the Ru surface, enhanced the Ru^{+} electron-deficient species. For this reason, selectivity of cyclohexane increases whereas conversion of benzene decreases. molar ratio of Zn/Ru decreased to 0.16 at 0.6 mol L^{-1} of NaOH, gives 89.3% of Cyclohexen selectivity and 45.3% benzene conversion. Furthermore, catalytic selectivity and activity was affected by excess addition of NaOH. Nedolivko et al. (2023) depicted various types of synthesis procedures (vacuum impregnation, incipient wetness impregnation, and impregnation under microwave irradiation) to obtain Ru-containing catalysts supported on halloysite aluminosilicate nanotubes (HNTs). The benzene hydrogenation reaction was studied at temperature 80^0C, H_2 pressure of 3.0 MPa, molar ratio of benzene to Ru=2000. Study shows that, Ru nanoparticles prepared by vacuum impregnation method were deposited into the internal cavity of aluminosilicate nanotubes whereas wetness impregnation method exhibits the formation of active phase on the external surface of halloysite. At last impregnation under microwave irradiation results uniform distribution of metal particles on the outer surface of HNT and determine an effective hydrogenation process to convert benzene to cyclohexane. Parsafard et al. (2020), had used co-impregnation method to obtain Ni/Zr-HMS/HZSM-5 (varying the amount of zirconium) catalyst which was then applied in benzene hydrogenation process. Fixed bed reactor was assessed to investigate the catalytic performance within the temperature range of about 130-190^{0}C. The study shows that Ni catalyst with Si/Zr = 35 provides better result in terms of stability, good catalytic performance and selectivity based on a long-term performance. Mohammadian et al. (2020), worked on benzene hydrogenation within the temperature range of 150-210^{0}C using a bimetallic nickel catalyst. Co-impregnation method was used for the

synthesis of bimetallic catalyst and the main aim of this work is not only to reduce carcinogenic effect but also to produce valuable products through improving the quality of fuel (octane number). Furthermore, the study also investigated some factors like reaction temperature and promoter type to understand the selectivity, specific rates and activity of the catalysts. NiAg/Zr-Kit-6-13X, NiMo/Zr-Kit-6-13X catalysts provide best selectivity and conversion at 150^0C and 170^0C respectively. Cuevas-García et al. (2021), had used various synthesis methods like ion exchange (IE), incipient wetness impregnation (IWI) and deposition precipitation (DP) to obtain Nickel catalyst supported on mordenite zeolite (same nickel content of 2wt%). All of the catalysts were studied based on their selectivity and conversion in hydrogenation of naphthalene with or without thiophene in the feedstock. In spite of lower nickel content, three of the catalysts represents higher conversion of naphthalene upto 94%. In this case, Ni-IE catalyst showed deactivation and products were related to acid base reaction but possess good activity. On the other hand, Ni-IWI deactivate fast and exhibits high selectivity for tetralin. Ni-DP was considered for higher hydrogenation activity and deactivate slowly as compared to other catalysts. Shubina et al. (2017), investigated hydrogenation of benzene using an Inerton-supported on nickel catalyst. Author also studied properties of the catalysts under different reaction conditions. Furthermore, rate constant (varying temperature), activation energy and conversion had been determined in this work. Li et al. (2016), had studied the hydrogenation of pyrolysis gasoline using an oxidic tri metallic Ni-Mo-Zn/Al_2O_3 and reduced passivated Ni catalyst (RP) and sulfided catalyst (RPS). Pre-sulphided treatment was applied to the catalyst in order to prevent thermal run-away during the beginning of the hydrogenation of pyrogasoline. A fixed-bed reactor (reaction temperature 30-70^0C, weight hourly space velocity (WHSV) 2.0 h^{-1}, at 2.8 MPa hydrogen pressure and volume of H_2/pyrogasoline = 200:1) was used to investigate the catalytic performance. Results showed that rising temperature of RPS catalyst was almost

20^0C lower as compared to Ni-Mo-Zn/Al_2O_3 catalyst and exhibited better stability (during initiation period) as well as selectivity in long-term operation. Dietzsch et al. (2000), suggested that conversion of benzene to valuable products such as cyclohexane impose an industrial interest due to the substitution of benzene in gasoline by other non-polluting components. Therefore, gas-phase catalytic hydrogenation of benzene was performed (at atmospheric pressure) to develop catalysts as an alternative to be used in liquid-hydrogenation. Ru containing catalysts with different support materials and Ru-coated catalysts (electrolytically formed alumina support) were investigated. Selectivity of Ru-coated catalysts was up to 45% whereas Ru-supported catalysts gave selectivity of 35% with conversion degrees of benzene 5%. Furthermore, performance of the catalysts were improved by increasing the partial pressure of hydrogen and methanol and also by the addition of second metal (copper) inside the oxide layer of coated catalysts. Rostamikia et al. (2019), had investigated the hydrogenation of benzene in the refiner platformate using Ni catalyst. A continuous fixed-bed reactor was considered for the study and its operating temperature was about 473-423K, under atmospheric pressure. Mainly two methods such as sol-gel and sedimentation were used for the synthesis of nickel catalysts and their activities were studied based on space velocity and molar ratio of H_2/Benzene. Catalyst prepared by sedimentation method gave highest conversion of benzene at 448K. Roy et al. (2013), reported a kinetic study of hydrogenation of toluene over Pt(0.15 wt.%)-Pd(0.15 wt.%)/Zr-HMS and Pt(0.15 wt.%)-Pd(0.15wt.%)/HMS catalysts in a continuous-upflow catalytic fixed-bed reactor. Here, hexagonal molecular sieve and Zr-HMS were synthesized and used as a support material in the hydrogenation process. Weight hourly space velocity (WHSV), temperature and hydrogen pressure were varied in order to study the activity of the catalysts. The study further shows that, conversion is dependent upon temperature and gives a well-defined maximum value. Pt(0.15wt.%)-Pd(0.15wt.%)/Zr-HMS catalyst showed an effective performance compared to

Pt(0.15wt.%)-Pd(0.15wt.%)/HMS catalyst in the hydrogenation of toluene. Ishii et al. (2021), investigated upon the effective use of support materials and its effect on improving the activity of catalyst. So, a great understanding was build up about the interactions between metal catalyst and support along with the surface characteristics. Carbon plays an important role in case of support material because of its higher electro conductivity, chemical and thermal stability. Moreover, surface properties of carbon compound can be controlled by doping hetero atoms. The study mainly focuses upon to investigate the support effect and activity of the catalyst (metal particles supported on heteroatom-doped carbon materials). N and B were introduced into the carbon-supported Ni particles in order to enhance its catalytic activity. Results show that, adsorption energy of the reactant on Ni gets changed leads to the improvement of Ni catalytic activity. Sassykova et al. (2017), investigated upon the hydrogenation of benzene ring in a gasoline fraction of Atyrau Oil Refinery LLP (Kazakhstan). Mainly mono- and bimetallic- catalysts were synthesized based on platinum metals. It was succeeded to disbar the benzene content from final sample or to decreases its quantity upto 0.06% and also to reduce the content of aromatic compounds around 0.6-4.65%. Further, benzene content was reduced to 0.16 wt% (initial sample contain 5.17 wt.%) along with the conversion was upto 97%. Amount of aromatic compounds for the "stable catalysate" was reduced from 51.6 to 22.95 wt.%. Thus, the catalytic hydrodearomatization of gasoline leads to the reduction in octane number. In the present work transition metal nickel (Ni) supported on aluminium oxide or alumina (Al_2O_3) has been explored as a hydrogenation catalyst. Benzene was considered as a representative compound to simulate the aromatics in jet engine or diesel fuels. Reason is that, catalytic hydrogenation of benzene is a bit tricky process as compared to other hydrocarbons. Hydrogenation activity of benzene over (2 wt%)Ni/γ-Al_2O_3 catalyst was studied in a continuous-upflow high pressure fixed bed reactor. Here, temperature and pressure were varied while keeping the liquid hourly space

velocity (LHSV) constant. Very few works have been reported over (2 wt.%)Ni/γ-Al_2O_3 catalyst (synthesized using ESI method) in catalytic benzene hydrogenation process. Thus, the main aim of this work is to study the performance and activity of Ni catalyst supported on γ-Al_2O_3.

CHAPTER 3

EXPERIMENTAL PROCEDURE

CHAPTER 3

EXPERIMENTAL PROCEDURE

3.1. Chemicals

3.1.1. Nickel (II) Nitrate Hexahydrate (Ni $(NO_3)_2$. $6H_2O$)

Transition metals are mainly considered for catalysts synthesis as it has a vacant d orbital. Here, the precursor material Nickel (II) Nitrate Hexahydrate is taken to obtain the Ni particles which will provide the active sites of the catalyst. Nickel (II) Nitrate Hexahydrate precursor material is highly soluble in water which will helps to make the solution possible easily. Another advantage of Nickel (II) Nitrate Hexahydrate precursor material is that, during calcination process metal oxide (NiO) is obtained, which leads to an active component for catalyst.

3.1.2. γ-Alumina (Al_2O_3)

Here, γ-Alumina (Al_2O_3) is taken as a support material over which the Ni particles will be dispersed to provide active sites. Main reasons of choosing γ-Alumina are due to its higher surface area and promote good dispersion of active metal species on its surface. γ-Alumina also shows an excellent chemical stability at high pH levels which means that, γ-Alumina does not go under any degradation during preparation method. γ-Alumina can withstand higher temperature effect and the structural properties does not change during reaction at high temperature.

3.2. Synthesis equipment's

3.2.1. Magnetic hot plate

Magnetic hot plate is used in order to enhance mixing efficiency during preparation of the solution.

3.2.2. Hot air oven

Used to remove water present in the solution at a temperature 100^0C.

3.3.3. Calcination chamber

Calcination chamber is used to remove the residual solvent (water) after drying process. Another reason is to decompose the nitrate ions into nitrate oxides to create the active sites for the catalyst. Since, calcination process is operated at higher temperature (400-450^0C), it stabilizes the structure of Ni/γ-Al_2O_3 catalyst.

3.3. Catalyst Synthesis

Excess solution impregnation method was used to prepare the Ni/**γ**-Al_2O_3catalyst. Here, metal precursor Nickel (II) Nitrate Hexahydrate was used and **γ**-Al_2O_3 was used as a catalyst carrier to obtain (2wt.%)Ni/Al_2O_3 catalyst. All the syntheses were conducted using double distilled water and the amount of nickel salts required to obtain specific catalyst such as, (wt.%)Ni was determined from stoichiometry. Desired concentration of Ni salt was added to 20g preheated alumina (γ-Al_2O_3) support (kept at 100^0C for 30 min) and stirred for 4 hr at pH: 8-9. Thereafter, slurry was kept in a hot air oven at 100^0C for 12 hr, and then calcined at 400-450^0C for 4 hr in an air flow.

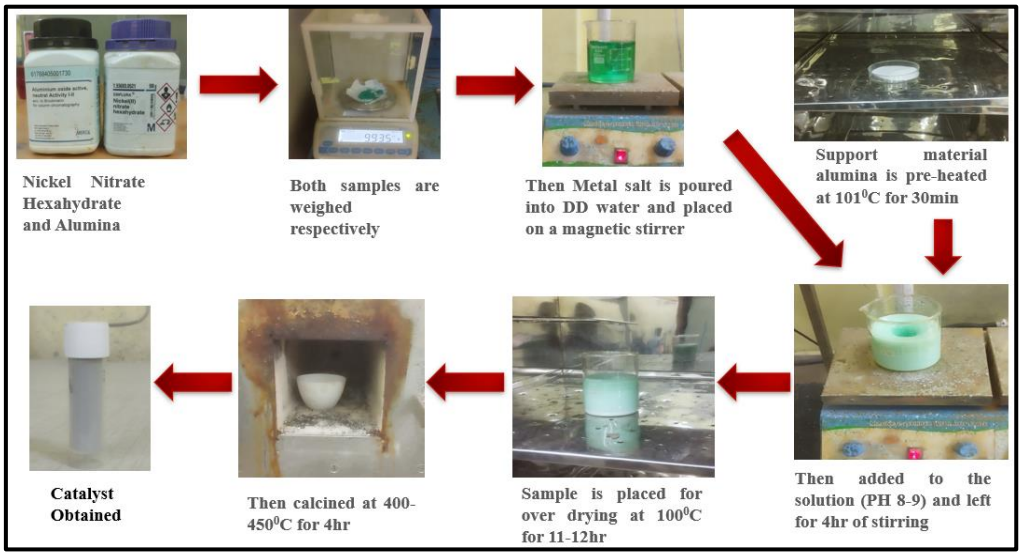


Fig.16. Preparation of (2 wt.%)Ni/γ-Al_2O_3 by ESI method

Thus way, deposition of precursor materials on the γ-Al_2O_3 support was successfully obtained. The calcined catalyst was further reduced using hydrogen gas in-situ.

3.3. Catalyst activity testing setup

The catalytic hydrogenation of benzene was performed in a high pressure continuous up-flow fixed bed reactor. The rector is made of SS316 and the length of the reactor is 50 cm and diameter of the reactor is 1.5 cm. The reactor was equipped with high pressure piston pump, with the ability to operate up to 180 bar pressure and 600^{0}C. Benzene hydrogenation was carried out under various conditions by changing reaction temperatures (270-390^{0}C), pressure (5-25 bar) and liquid hourly space velocity (LHSV) of feed at 2 min^{-1}. Before the hydrogenation reaction the (2wt.%)Ni/Al_2O_3catalyst was reduced in-situ at 230^{0}C for 1hr over a continuous flow of a mixture of gases (hydrogen and nitrogen).Benzene was pumped by HPLC pump and sent it to the vaporizer (at temperature 200^{0}C) to vaporize the liquid benzene feed.

Hydrogen gas was sent to the mixer unit by a flow controller at 50 bar, where vapor phase of benzene and hydrogen mixed with each other. After that, the gas mixture containing hydrogen and benzene vapor was further passed through a pre-heater at temperature 300^0C, and finally fed into the reactor. 11g of calcined (2 wt.%)Ni/Al_2O_3catalyst was loaded at the centre of the reactor and remaining spaces of the reactor (bottom and top parts) were filled with glass beads of 2.1-3 mm diameter and glass wool in order to fix the catalyst particles and also to prevent the entry-exit effect of the reactor. Plug flow conditions were maintained throughout the experiment.

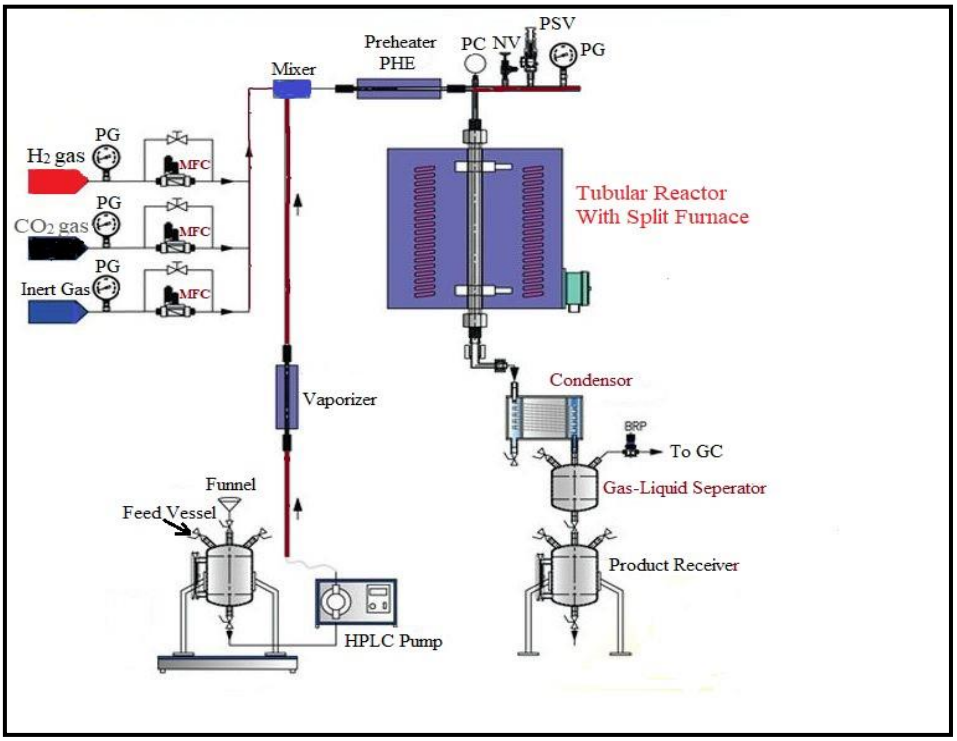


Fig.17. Schematic diagram of continuous-upflow high pressure and temperature reactor

The products from the outlet of the reactor were condensed and passed to a gas-liquid separator (GLS). Then, gas phase was sent to gas bomb and the liquid products were collected in a vial from liquid vessel. The liquid products were then analysed using Gas-

Chromatography Mass Spectrometer (GCMS). Activity of the catalyst is demonstrated in terms of hydrogenation of benzene using specific reaction rate as follows

$$r_i = \frac{X_i F}{W_{cat}} \quad \ldots\ldots\ldots\ldots\ldots\ldots (1)$$

X_i = conversion of benzene, r_i= specific reaction rate ($gmol/g_{cat}.min$), W_{cat}= weight of catalyst (g).

3.4. Characterization techniques

3.4.1. Brunauer, Emmette and Teller analysis (BET)

BET analysis is mainly used for the determination of surface area for porous material, particularly adsorbents, solid catalyst and nanoparticles. In 1938, three scientists Stephen Brunauer, Paul Hugh Emmett, and Edward Teller had developed a theory to determine surface properties of materials, known as BET theory and they published the first article about BET theory in the Journal of American Chemical Society. The physical significance of BET analysis tells us about the adsorption of N_2 gas molecules on the surface a solid material. Based on BET theory, when a gas molecule is adsorbed on the surface of a solid material (at constant temperature 77K), a monolayer formation will occur. In this analysis, amount of gas adsorbed (cm^3/g) as a function of relative pressure ($\frac{P}{P_0}$) is measured. After the formation of monolayer, it is assumed that a formation of multilayer over the monolayer on the surface of a catalyst will occur and based on the pattern we can understand the type (Type I-IV) of adsorption-desorption. Following steps are involved in BET analysis.

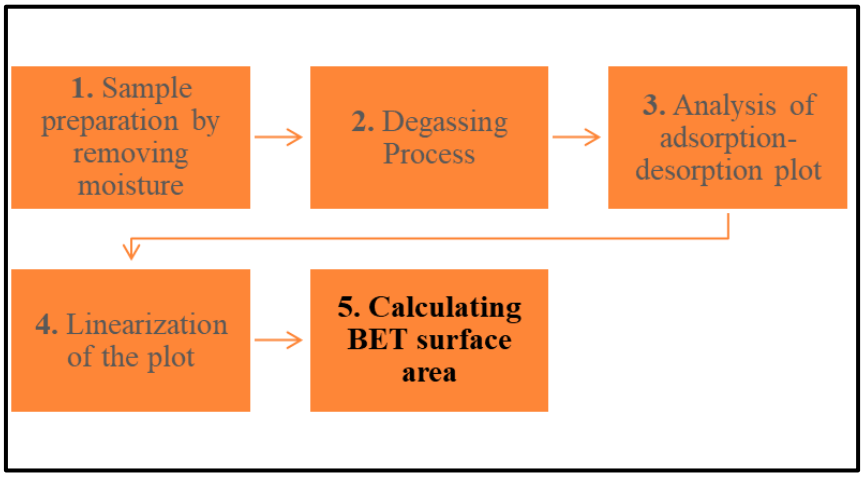


Fig.18. Steps required for BET analysis

The BET analysis includes a non-reactive probing gas N_2 which is first allowed to get adsorbed on a catalyst surface at high pressure. A reversible process physisorption is preferred, as it can be easily carried out without causing any transition to the microstructure of the porous material. Fig.22 represents the BET instrument which is used in this study

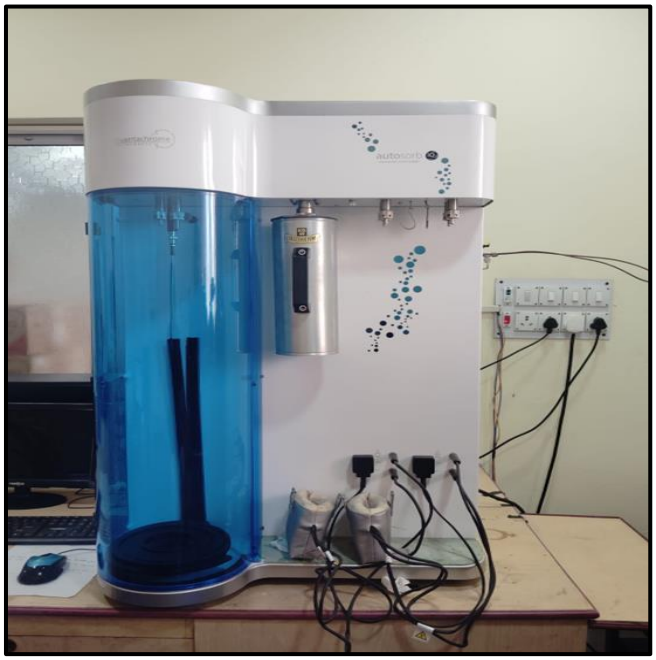


Fig.19. BET analyser (Autosorb iQ, UGC SAP laboratory, Chemical Engg. Dept., JU)

Sufficient time duration (4-5 hr) has been given in order to achieve an effective adsorption over the surface of catalyst. After that, we gradually lower the pressure and slightly increases temperature to favour the desorption process. During the increases in temperature, top layer of physisorbed N_2 gas molecules starts to break the van de Waals bond and then released. Here, the desorbed probe gas molecules are directed towards mass spectrometer or gas flowmeter, which helps to determine the number of desorbed gas molecules

Table.5. Specifications of the BET analyser and operation conditions are given below

Instrument	Autosorb iQ Station 2
Software	AsQinn
Catalyst studied	(2 wt.%)Ni/γ-Al_2O_3
Sample weight	0.8679 g
Adsorbate	N_2 gas
Bath temperature	77 K
Outgas temperate	377 K

3.4.2. Thermogravimetric analysis (TGA)

Thermogravimetric analysis is a technique used for the analysis of change in mass of a solid material as a function of time or temperature, in a controlled atmosphere. In other words, TGA is an excellent method to investigate the relationship between temperature and the physical and chemical changes that occur within the materials during decomposition or in a particular reaction. In TGA, a small sample of material is subjected under a controlled temperature range in a specially designed furnace, which is then weighed with the help of a balance system. In case of thermal stability of a material, TGA analysis determines the temperature at which decomposition of the materials or participation in reaction takes place.

The physical significance of TGA analysis refers to provide valuable information regarding thermal stability and behavior of a material. Further, TGA analysis also offers to identify the presence of volatile components, which is monitored by the mass loss within a specific temperature range. The following steps are involved in TGA analysis, which is given below.

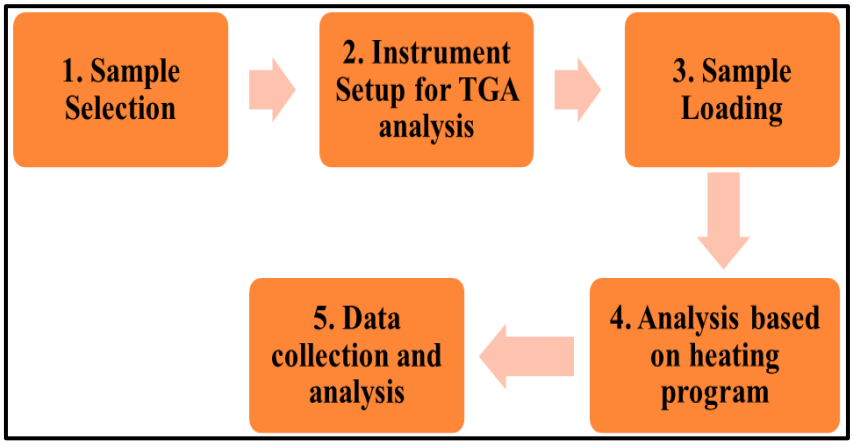


Fig.20. Steps involved in TGA analysis

This helps to understand the mechanism as well as reaction pathways to design and optimize a reaction. At last, TGA also effective in order to study phase transition such as, crystallization, melting and glass transition, takes place due to the degradation of mass.



Fig.21. Thermogravimetric analysis instrument to study the decomposition of a material within in a temperature range 40-800^{0}C

The picture of TGA instrument (PerkinElmer STA 6000) used in this study is given below Depending upon the analysis and characteristics of the same material being studied, respective stepwise or linear temperature ramp has to be chosen. In TGA analysis, the heating process carried out in the presence of reactive gas to prevent oxidation and other chemical reactions or under an inert atmosphere (such as argon or N_2 gas). Another application of TGA analysis includes the study of kinetics during the degradation of mass of a material as function of temperature or time.

CHAPTER 4

RESULTS AND DISCUSSIONS

CHAPTER 4

RESULTS AND DISCUSSIONS

4.1. Catalyst Characterization

4.1.1. Brunauer, Emmette and Teller analysis (BET)

In this study, (2 wt.%)Ni/γ-Al_2O_3 catalyst was degassed at 300^0C for 3.5 hr under vacuum condition (10-5 mbar) prior to adsorption experiment. Fig 24 represents the N_2 adsorption-desorption isotherms and pore size distribution of prepared catalyst (2 wt.%)Ni/γ-Al_2O_3. Mainly four types of isotherms curves are involved in BET analysis in order to understand the N_2 adsorption-desorption pattern. Type I to III isotherm curves represent nonporous materials whereas, Type IV and V represents porous material. The shape and structure of the sample material can be understood from hysteresis loop. Here, the N_2 adsorption-desorption isotherm graph indicates a type IV isotherm pattern for the catalyst and typically a mesoporous material of surface area 24.79 m^2/g. According to international union of pure and applied chemistry (IUPAC) classification, the isotherm graph shows hysteresis loop of type H2. Here, the pores of the catalyst can have uniform shape or size. Both the isotherms possess clear loops and abrupt hysteresis covering P/P_0 within the range of 0.4 to 0.6. Here, the desorption curve is higher than the adsorption curve within the range of relative pressure 0.5-0.95. Reason is that, whenever the pressure of a gas decreases over a solid surface, desorption simultaneously increases. Since, the process itself is an adsorption rather than absorption, at first with increasing pressure the adhesion of N_2 molecules occur over the surface of material at a very slow rate as it can be seen from the graph and whenever pressure surrounding the adsorbed N_2 molecules becomes lower desorption takes place at a higher rate.

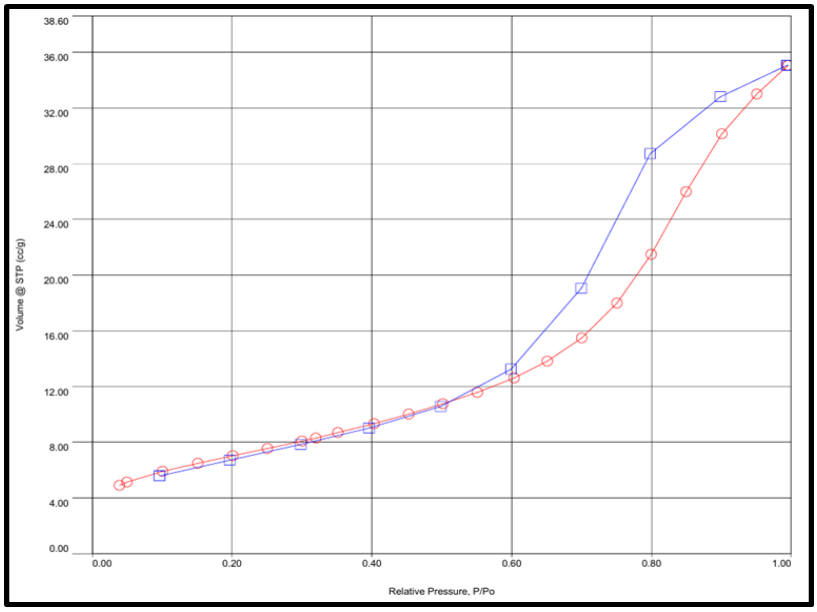


Fig.22. N_2 adsorption-desorption isotherm of (2 wt.%) Ni/γ-Al_2O_3

The adsorption-desorption is similar for both catalyst and support, which shows that the structure of γ-Al_2O_3 does not affect after impregnation with Ni metal. However, during the impregnation of this metal species can block some of the pores of γ-Al_2O_3 which can cause the declining of hysteresis zone on the N_2 adsorption-desorption curves of the catalyst. This approved a well-established impregnation of Ni metal on the γ-Al_2O_3 surface. Manukyan et al. (2015), obtained the surface area for (10 wt.%) Ni/Al_2O_3 around 110 m^2/g. As compare to the BET surface area in this study, the catalyst (2 wt.%) Ni/γ-Al_2O_3 shows an effective dispersion of Ni metal particles over the surface of γ-Al_2O_3. Jiang et al. (2020), also studied the BET surface area of cordierite monolith (used as a catalyst) in acid treatment gives 20 m^2/g of surface area, which is lower compare to (2 wt.%)Ni/γ-Al_2O_3. Liu et al. (2015), had found out the surface area of Ni/Al_2O_3 around 44 m^2/g, where higher amount of support material alumina was taken. Wang et al. (2009), showed the BET surface area of RuO_2/TiO_2 catalyst was around 18 m^2/g, which is lower as compared to (2 wt%) Ni/γ-Al_2O_3 catalyst in this study.

In order to determine the surface area (m^2/g) of a material, the BET equation is used which is given below and the calculations to determine BET surface area are given on Appendix B.2.

$$\frac{p}{V(p_0 - p)} = \frac{1}{V_m.c} + \frac{c-1}{V_m.c}\frac{p}{p_0} \quad \ldots\ldots\ldots\ldots\ldots\ldots (2)$$

$$V_m = \frac{1}{(\text{Slope}+\text{Intercept})} \quad \ldots\ldots\ldots\ldots\ldots\ldots\ldots\ldots (3)$$

$$S_T = \frac{V_m \,.\, N \,.\, S}{v} m^2 \quad \ldots\ldots\ldots\ldots\ldots\ldots\ldots\ldots (4)$$

$$S_{BET} = \frac{S_T}{a} \quad \ldots\ldots\ldots\ldots\ldots\ldots\ldots\ldots (5)$$

Where, V_m = monolayer volume in cm^3, N = Avogadro's No. (6.023×10^{23}), S = Cross-sectional area of a N_2 molecule (0.162 nm^2), v = molar volume of N_2 (22.4 L), V = amount of liquid N_2 adsorbed in cm^3/g of catalyst, p = vapour pressure of N_2 on the surface of material, p_0 = Pressure at STP 1 atm or 760 mmHg, c = BET constant, S_T = total surface area (m^2), S_{BET} = BET surface area of the material (m^2/g).

4.1.2. Thermogravimetric analysis (TGA)

Fig 30 represents the TGA analysis of (2 wt%) Ni/γ-Al_2O_3 within the temperature range of 40-800^{0}C. The Y-axis of the plot represents percentage weight loss (wt%) of the catalyst material whereas, X-axis represents the temperature range (^{0}C). The graph shows mainly two degradations of mass, where the first one ranges from 36-120^{0}C and the second one ranges 125-500^{0}C. At the initial stage of TGA analysis for (2 wt.%) Ni/γ-Al_2O_3 catalysts shows a degradation of mass about 1.8% within the temperature range 36-120^{0}C. The reason of this initial degradation in mass is mainly due to desorption water molecules from the surface of the catalyst.

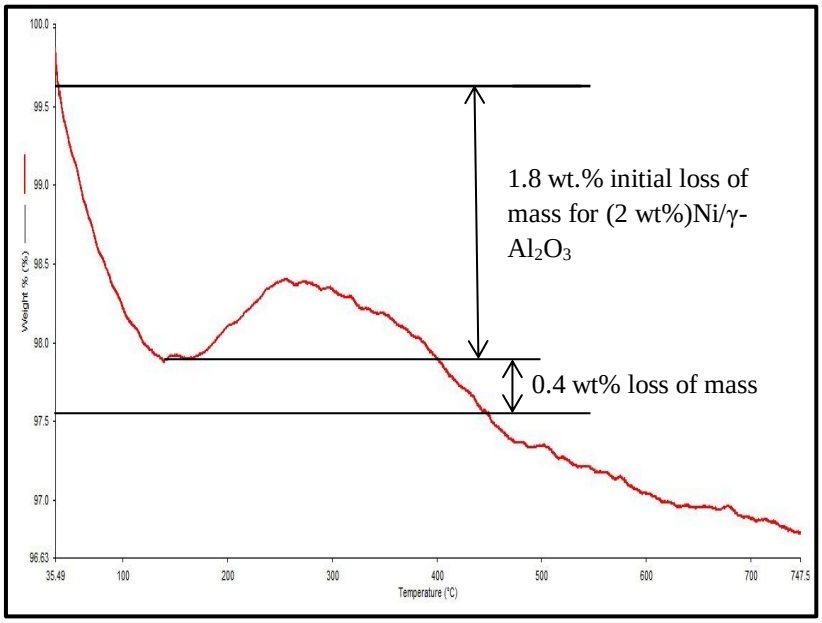


Fig.23. TGA curve of fresh (2 wt%) Ni/γ-Al_2O_3 catalyst

Since, alumina has a tendency to adsorb water so, desorption of water molecules takes place at lower temperature (<150^0C). Furthermore, within higher temperature range 125-500^0C the degradation in mass is almost around 0.4%, which is lower as compared to the initial stage. The decomposition at higher temperature can cause due to sudden occurrence of phase transition or for the rearrangement of atoms. Nickel species present in the catalyst can undergo oxidation reaction at higher temperature during TGA analysis. Since, the weight loss is much lower, later explanation is not valid in this case. Awad et al. (2017), had showed the TGA analysis of Ni/Al_2O_3 catalyst used for hydrogen production. The TGA graph shows a degradation of mass within the temperature range 500-720^0C is of higher side. Almost 9.1% of mass decomposition takes place for Ni/Al_2O_3 catalyst, which is higher as compared to (2 wt.%) Ni/γ-Al_2O_3 catalyst used in this study. Isha et al, (2020), had showed almost 28% mass decomposition of Ni/Al_2O_3 catalyst within the higher temperature range 200-320^0C.

4.2. Effect of parameters

4.2.1. Effect of Temperature on Benzene conversion

At an elevated temperature the structure of mesoporous material disintegrates, which is one of the limitations of mesoporous material to use it as catalyst. In order to understand the activity of synthesized material such as (2wt.%)Ni/γ-Al_2O_3 was tested in benzene hydrogenation. During the hydrogenation reaction of benzene cyclohexane was found to be the main product.

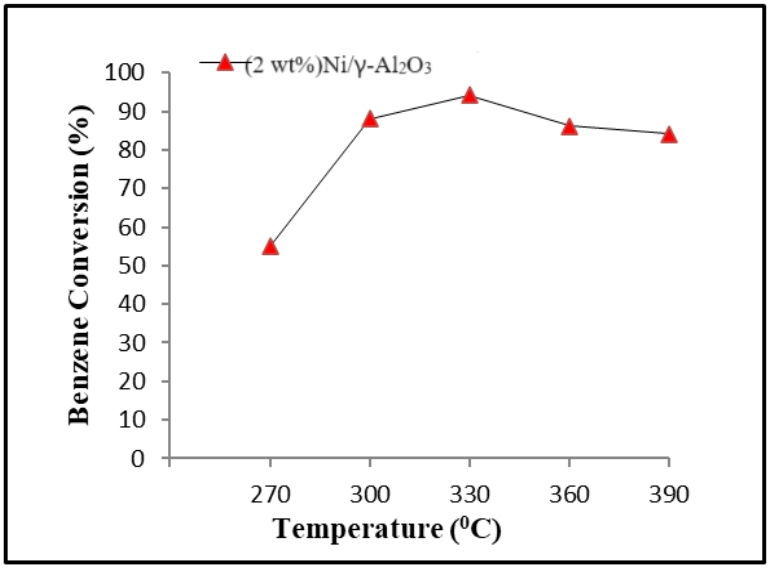


Fig.24. Influence of temperature on benzene conversion at H_2 pressure = 25 bar, feed LHSV = 2 min^{-1}

At reaction temperature 270^0C, Benzene conversion was found to be 55%. After that, increasing the temperature of the hydrogenation reaction, benzene conversion also increases and at 330^0C, 15 bar hydrogen pressure and LHSV= 2 min^{-1} maximum conversion of 94.16% was achieved using (2 wt.%)Ni/γ-Al_2O_3 catalyst. Increasing in benzene conversion within the temperature range 270-330^0C is due to the fact that, at higher temperature the kinetic energy of the reactant molecules increases which leads to enhance the reaction rate. Also, at higher temperature activation energy gets lower and makes the hydrogenation reaction easier to

proceed. Beyond 330^{0}C, slightly decrease in benzene conversion up to 84.14% can be observed. Higher temperature can shift the position of thermodynamic equilibrium of the reaction for which the conversion gets lower (Park et al., 2023). On the other hand, at higher temperature surface coverage of hydrogen gets lower and the active sites of the catalyst becomes saturated with benzene which decreases the conversion to obtain cyclohexane.

Rate constants were determined from experimental data and lnk vs 1/T is plotted as shown in fig.28 for (2 wt%)Ni/ γ-Al_2O_3.

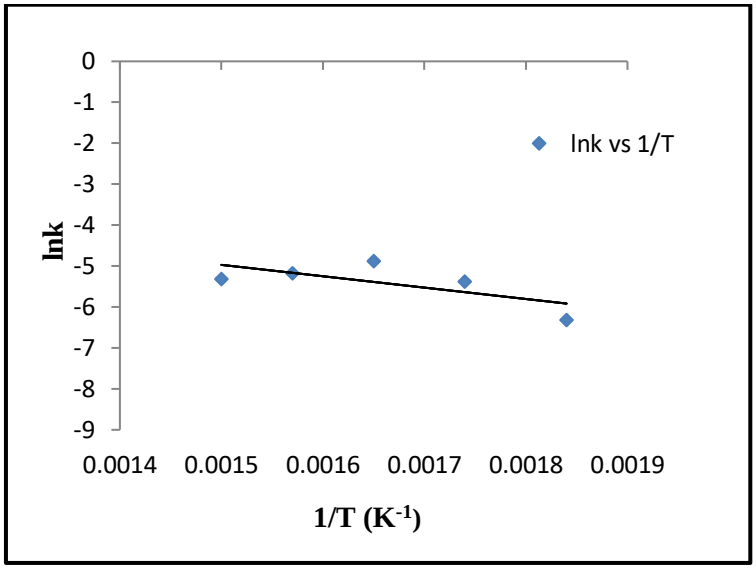


Fig.25. Arrhenius plot of ln(k) as a function of 1/T for (2 wt%)Ni/γ-Al_2O_3 catalyst

The activation energy of the benzene hydrogenation reaction using (2 wt.%)Ni/ γ-Al_2O_3 catalyst was around 23.24 KJ/mol. The calculation based on activation energy has been shown on Appendix B.3. As the value of activation energy for (2 wt.%)Ni/ γ-Al_2O_3 catalyst is slightly on the lower side, indicates the presence of higher activity of (2 wt.%)Ni/ γ-Al_2O_3 catalyst. The calculated activation energy from the present study is compared with the activation energy described in literature for hydrogenation of benzene. Navarro et al. (2000), obtained the value of activation energy around 128.3 kJ/mol using Pt-Pd/silica catalyst at

513K. Sayes et al. (2004), reported the value of activation energy was around 104 kJ/mol using Pt(111) catalyst in a benzene hydrogenation reaction. It can be seen that, activation energy E_a using (2 wt.%)Ni/γ-Al_2O_3 catalyst is almost two-third to half of the reported value of activation energy in literature. This is due to the fact that, hydrogenation reaction was carried out in the presence of catalyst, which makes the reaction easier to proceed by different pathways with a low energy barrier.

4.2.2. Effect of H_2 pressure on Benzene conversion

Fig.29 represents the plot of Benzene conversion at 390^0C as a function of hydrogen pressure. From the figure it can be observed that benzene conversion increased with hydrogen pressure upto 15 bar beyond which it slightly decreases to 25 bar. Initial increase in benzene conversion from 5 bar to 15 bar can be considered as a fact that, due to the increase in pressure within this pressure range enhanced the adsorption of benzene on the active sites of the catalyst which leads to the increase in benzene conversion.

Here, hydrogen also gets adsorbed with benzene and takes part in the reaction and due to its smaller size, hydrogen diffuses much faster as compared to benzene. Thus, there exist competing reactions where hydrogen engaged with the active sites and dissociates into atomic hydrogen to participate in the reaction. So, the adsorption, diffusion and activation of hydrogen lower the benzene conversion (Roy et al., 2013). The phenomenon can be explained with the help of Lweis and Bronsted acidity where presence of hydrogen decreases the Bronsted acidity for which concentration of intermediates also get reduced, results in lowering the benzene conversion.

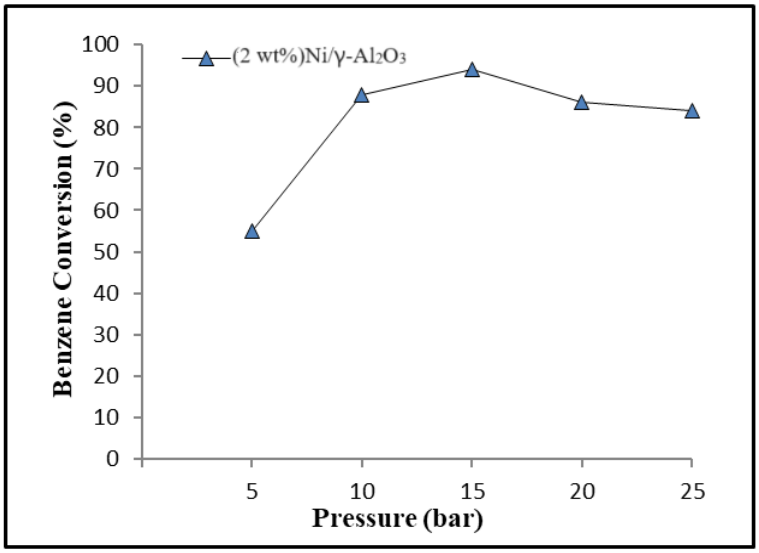


Fig.26. Influence of H_2 pressure on benzene conversion at temperature = 390^0C, feed LHSV = 2 min^{-1}

Roy et al. (2013), also found that the conversion of toluene increases with pressure effect and then remains constant after 20 bar H_2 pressure. Ning et al. (2006), had also studied the effect of H_2 pressure on benzene conversion. The study showed the highest conversion of benzene at 7 bar and after that slightly decreases.

4.2.3. Effect of Feed Liquid Hourly Space Velocity on Benzene Conversion

Fig shows the effect of feed LHSV on the conversion of benzene at 663 K temperature and 20 bar pressure. As it can be seen from plot, the conversion of benzene is highest at LHSV = 1 min^{-1} and along with the increase in feed flow rate benzene conversion decreases to 65% at LHSV = 4 min^{-1}. So, the conversion of benzene was found to decrease with an increase in LHSV of benzene, which consists of two different explanations. Increasing the liquid flow rate, wetted fraction of the catalyst as well as the liquid-solid and gas-liquid mass transfer coefficients increases.

On the other hand, at lower liquid flow rate, catalyst particles are partially wetted for which the benzene conversion increases due to the direct deposition of gas phase reactant on the catalyst surface and already wetted internally due to capillary forces. Therefore, increase in liquid flow rate is expected to retard the increase in conversion, whereas an increase in external mass transfer coefficient enhances the conversion. Another possible reason for the decrease in conversion is due to the shorter residence time of gas phase reactants inside the reactor under high feed LHSV.

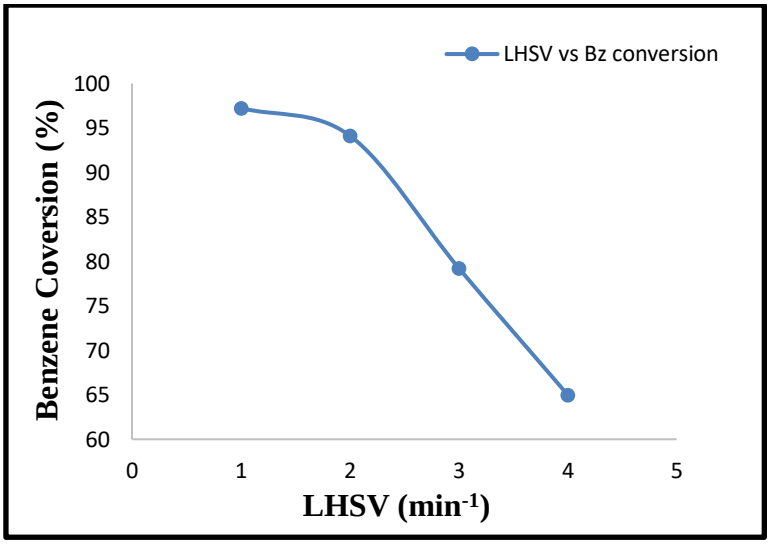


Fig.27. Benzene conversion vs LHSV plot at pressure 20 bar and temperature 663K

The former explanation is applicable for the large catalyst bed, but in this study much lower amount of catalyst around 11g (smaller catalyst bed) was considered, so the latter explanation is more effective for this study. Roy et al. (2013), had showed the effect of WHSV on toluene conversion and depicted decrease in toluene conversion with respect to WHSV, which is similar with this study. Mostafa et al. (2019), also depicted the decreases in benzene selectivity (%) as a function of LHSV, where benzene selectivity decreases from 62-23% at LHSV = 4 min^{-1}. Gheni et al. (2016), had studied on the effect of LHSV on benzene content in percentages. The study shows an initial decrease in benzene content (5-2wt%) within the

LHSV range 1-1.25 hr^{-1}. After that, the benzene content slightly increases to 3wt% at LHSV 2 hr^{-1}. The reason is due to the thermodynamic equilibrium shifting towards backward reaction, whereas (2 wt.%)Ni/γ-Al_2O_3 catalyst in this study shows an effective thermal stability to prevent the backward reaction.

4.3. Modelling and kinetics of catalytic hydrogenation of Benzene

4.3.1. Power Law Model

Power law model was considered as a simplest form of kinetic equation. The rate constant and also the activation energy was determined in a separate experiment. Here, the order of H_2 and Benzene were determined with the help of Power law model, considering of the same experimental conditions which were described above. The reaction products were analyzed using GC as for the test of catalytic hydrogenation of benzene. To determine the reaction order of H_2 and benzene, Ni/γ-Al_2O_3 catalyst was examined within the temperature range of 270^0-390^0C for a reaction mixture containing (2 wt.%)Ni/γ-Al_2O_3 catalyst with 4 mL/min of Benzene flow rate and maintaining constant H_2 flow rate at 350 mL/min.

After each reaction (varying pressure, temperature and LHSV), catalyst was cleaned with H_2 flow at 350^0C and the whole integrated system was cleaned by flowing inert gas. In this condition, at a constant temperature of 390^0C, logarithmic representation of reaction rate (1/r) against H_2 pressure mostly follows a linear curve. Slopes of the curve represent the order of reaction based on individual components with varying the pressure of the catalytic fixed bed reactor.

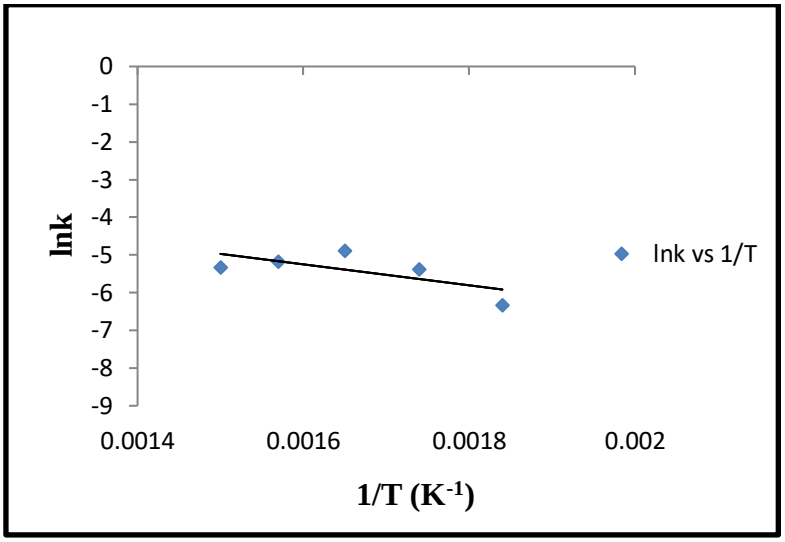


Fig.28. Arrhenius plot of ln(k) as a function of 1/T

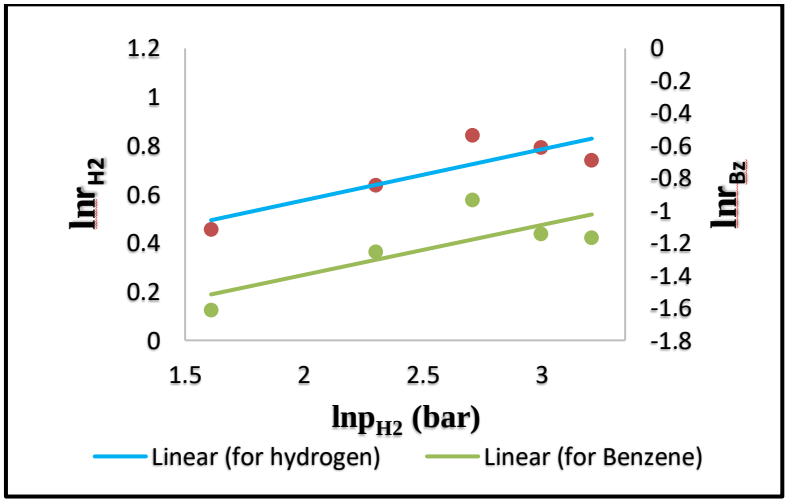


Fig.29. Estimation of Power Law Model to determine the order of Bz and H_2 at T = 390^0C,

feed flow rate = 8 mL/min

In this case, for kinetic studies, the reaction rate was defined as follows,

$$r = \frac{(\text{Bz flow rate} \times \text{Bz density} \times \text{Conversion})}{(\text{Mol.wt.of Bz} \times \text{Mass of catalyst} \times \text{Mass percentage of impregnated metal})} \quad \ldots\ldots\ldots (6)$$

Fig 32 shows the effects on reaction rate for benzene and H_2 due to the variation of H_2 pressure. The respective partial orders for benzene and H_2 were calculated using the following empirical kinetic equation,

$$r = k.\, p_{H_2}^{n}.\, p_{Bz}^{m} \text{ ……..…….... (7)}$$

Where, k is the rate constant and n, m are the orders of H_2 and benzene respectively. The reaction order of hydrogen on catalyst was measured 1.0 to 1.8 at constant temperature 390^0C, while for benzene was found 0.8 to 1.2. As can be seen in fig 32, the reaction rate of H_2 and benzene both increases with hydrogen pressure whereas the order of hydrogen and benzene tend towards 1st order reaction. This is due to substantial increases in surface coverage of each hydrogen and benzene molecules on the active sites of the catalyst. Further details about the calculation of order for H_2 and benzene are given in details in Appendix B.4.

Arrhenius plot was shown in fig.31 to determine the activation energy (E_a). Reaction order close to 1 shows a good fit to the experimental data. Temperature dependency of rate constant (k) was expressed in terms of logarithmic form of Arrhenius equation, and the best linear correlation can be obtained between logarithmic rate constant (ln k) and 1/T.

$$\ln k = \ln A - \frac{E_a}{RT} \text{ …… (8)}$$

The table given below shows the order of H_2 and Benzene

Where, r_{H_2} = rate of reaction for H_2, r_{Bz} = rate of reaction for benzene, n_{H_2} = order of H_2, n_{Bz} = order of benzene.

4.4. Reaction mechanism of hydrogenation of benzene over Ni/γ-Al_2O_3 catalyst

The hydrogenation of benzene using Ni/γ-Al_2O_3 catalyst is basically represents a complex reaction mechanism with various steps. The reaction mechanism mainly consists of five steps where the 1st is the adsorption of H_2 gas on the nickel catalyst and then the second step promotes the adsorption of benzene on the nickel catalyst. 3rd step of the reaction mechanism follows the hydrogenation reaction of benzene on the active sites of the nickel particles. After the completion of hydrogenation reaction step, desorption of some excess amount of H_2 and the product cyclohexane occurs in 4th and 5th step.

The reaction mechanism of catalytic hydrogenation of benzene (Bz) to cyclohexane (Cycl) is represented in the following series of events below-

1st step of reaction, $$H_2 \xleftrightarrow{\text{Ni Catalyst}} H_2(ads) \xleftrightarrow{\text{Ni Catalyst}} 2H(g)$$

2nd step of reaction, $$Bz(g) \xleftrightarrow{\text{Ni Catalyst}} Bz(ads) \xleftrightarrow{\text{Ni Catalyst}} Bz^*(ads)$$

3rd step of reaction, $$Bz^*(ads) + 6H(ads) \xleftrightarrow{\text{Ni Catalyst}} Cycl(ads) \xleftrightarrow{\text{Ni Catalyst}} Cycl(g)$$

$$6H \xleftrightarrow{\gamma-Al_2O_3} 6H^+ + 6e^-$$

$$Bz(g) \xleftrightarrow{\gamma-Al_2O_3} Bz(ads)$$

4th step of reaction, $$6H + Bz(ads) \xleftrightarrow{\gamma-Al_2O_3} Cycl(ads) \leftrightarrow Cycl(g)$$

$$6H + Bz(g) \xleftrightarrow{\gamma-Al_2O_3} Cycl(g)$$

5th step of reaction, $$2H \xleftrightarrow{Ni/\gamma-Al_2O_3} H_2$$

Here, the H_2 gas at first gets contact with the nickel catalyst, placed inside the reactor tube gets adsorbed and breaks the H_2 molecule to hydrogen atoms. Similarly, the vapor phase of

the benzene also gets adsorbed on the nickel sites and form an intermediate compound of benzene Bz^{*}. Then, both the intermediate compound Bz* and H atoms react to from cyclohexane (Cycl), which is then desorbed as a gas phase from the active sites of the catalyst.

CHAPTER 5

CONCLUSIONS AND FUTURE WORK

CHAPTER 5

CONCLUSIONS AND FUTURE WORK

5.1. Conclusions

The study shows an effective conversion of benzene (aromatic compound) to cyclohexane (unsaturated compound) using (2 wt.%)Ni/γ-Al_2O_3. The operating conditions and parameters for this reaction are-

Reactants	H_2 and benzene
Types of parameters in hydrogenation reaction of benzene	Temperature, pressure and LHSV effect on benzene conversion
Maximum operational condition	Pressure = 180 bar, T = 600^0C
Tested reaction conditions	Pressure = 5-25 bar, T = 390^0C and LHSV = 2 min^{-1}

Under the tested reaction conditions, 94.16% conversion of benzene to cyclohexane was successfully achieved using (2 wt.%)Ni/γ-Al_2O_3 catalyst. Benzene conversion measured at 390^0C, at LHSV= 2 min^{-1} was found to increase with pressure within 5-15 bar and after that the benzene conversion gets slightly reduced up to 25 bar due to the formation of saturation on the active sites of the catalyst. On the other hand, conversion of benzene increases with temperature upto 330^0C and then decreases. The reason is due to the existence of thermodynamic equilibrium at higher temperature reaction. Further, the study also focuses upon the effect of LHSV on benzene conversion, which shows a significant decrease within the range of LHSV 1-4 min^{-1}.

The activation energy of benzene hydrogenation reaction was found to be 23.24 kJ/mol using (2 wt.%)Ni/γ-Al_2O_3 catalyst which results a higher activity in terms of catalyst performance.

Since, the reaction temperature is on the higher side (390^0C), a stable catalyst is required in order to achieve an effective conversion of benzene. Here, TGA analysis shows that, (2 wt.%)Ni/γ-Al_2O_3 catalyst is highly stable and no structural changes occur as the weight percent loss is 0.4%. The BET analysis of this catalyst gives the surface area of about 24.79 m^2/g, which is an effective to provide the sufficient number of active sites. Furthermore, Power Law model shows that the reaction is of 1^{st} order for both H_2 and benzene. From Power Law model we can say, the experimental data points fit well with the theoretical equations and gives a linear plot. So, the catalyst (2 wt.%)Ni/γ-Al_2O_3 possesses stable activity, higher thermal stability with no significant amount of metal agglomeration during benzene hydrogenation and acts as an effective catalyst to convert benzene into cyclohexane.

5.2. Future Work

The hydrogenation of benzene involves several research directions and technological advancement. The selectivity of the catalyst (2 wt.%)Ni/γ-Al_2O_3 can be improved to maximize the formation of cyclohexane while minimizing the formation of by products like, cyclohexadiene. Only, 2 wt.% of Ni metal particle is considered in this study, whereas further increases in metal concentration will provide an improvement based on providing active sites and increasing surface area. Further, different types of support materials (zeolite, other oxide base support La_2O_3, TiO_2, SiO_2), bi-metallic and also tri-metallic catalysts needs to be studied further.

REFERENCES

Ahmed, E.M. Hydrogel: Preparation, characterization, and applications. *J. Adv. Res.* **2013**, 5, 2-16.

Al-Attas, T.A., Ali, S.A., Zahir, M.H., Xiong, Q., Al-Bogami, S.A., Malaibari, Z.O., Razzak, S.A. and Hossain, M.M. Recent advances in heavy oil upgrading using dispersed catalysts. *Energ. Fuel*, **2019**, 33(9), 7917-7949.

Alimohammadi, N. and Fatthi, S. Comparing the Performance of Heterogeneous Pd-Supported Catalysts: Pd/ZSM-5, Pd/13X and Pd/Al_2O_3 for the Hydrogenation of Benzene in a Mixture of Normal Heptane and Benzene. *Iran. J. Chem. Eng.* **2021**, 18(4), 3-19.

Biru, E.I., Necolau, M.I., Zainea, A. and Iovu, H. Graphene oxide–protein-based scaffolds for tissue engineering: recent advances and applications. *Polym. J.* **2022**, 14(5), 1032.

Chen, Z., Sun, H., Peng, Z., Gao, J., Li, B., Liu, Z. and Liu, S. Selective hydrogenation of benzene: Progress of understanding for the Ru-based catalytic system design. *Ind. Eng. Chem. Res.* **2019**, 58(31), 13794-13803.

Cuevas-García, R., Téllez-Romero, J. G., Ramírez, J., Sarabia-Bañuelos, P., Puente-Lee, I., Salcedo-Luna, C., ... & Nolasco-Arizmendi, V. A. Effect of the preparation method on particle size and reaction selectivity on naphthalene hydrogenation over Ni/H-MOR catalysts. *Catal. Today* **2021**, 360, 63-71.

Dey, S. and Mehta, N.S. Synthesis and applications of titanium oxide catalysts for lower temperature CO oxidation. *Curr. Res. Green Sustain. Chem*. **2020**, 3, 100022.

Di Marcoberardino, G., Binotti, M., Manzolini, G., Viviente, J.L., Arratibel, A., Roses, L. and Gallucci, F. Achievements of European projects on membrane reactor for hydrogen production. *J. Clean. Prod.* **2017**, 161, 1442-1450.

Ding, Y., Dong, Y., Zhang, H., Zhao, Y., Yang, M. and Cheng, H. A highly adaptable Ni catalyst for Liquid Organic Hydrogen Carriers hydrogenation. *Int. J. Hydrog. Energy.* **2021**, 46(53), 27026-27036.

Feng, Y. H., Bai, X., Wei, X. Y., Dilixiati, Y., Shen, J., Li, L., ... & Kang, Y. H. Solvent-mediated selective hydroconversion of benzyloxybenzene over a Ni/β_{40} catalyst. *Fuel. Process. Technol.* **2023**, 252, 107963.

Gheni, S.A., Jarullah, A.T. and Razak, G.H.A. Naphtha catalytic upgrading for production of environmentally-friendly gasoline. *J. Chem. Eng. Process Technol.* **2016**, 7, 303.

Girgis, M.J. and Gates, B.C. Reactivities, reaction networks, and kinetics in high-pressure catalytic hydroprocessing. *Ind. Eng. Chem. Res.* **1991**, 30(9), 2021-2058.

Glotov, A., Stavitskaya, A., Chudakov, Y., Ivanov, E., Huang, W., Vinokurov, V., Zolotukhina, A., Maximov, A., Karakhanov, E. and Lvov, Y. Mesoporous metal catalysts templated on clay nanotubes. *B. Chem. Soc. Jpn.* **2019**, 92(1), 61-69.

Glotov, A., Stytsenko, V., Artemova, M., Kotelev, M., Ivanov, E., Gushchin, P. and Vinokurov, V. Hydroconversion of aromatic hydrocarbons over bimetallic catalysts. *Catal.* **2019**, 9, 384; 10.3390/catal9040384

Haider, H.I., Zafar, I., Ain, Q.U., Noreen, A., Nazir, A., Javed, R., Sehgal, S.A., Khan, A.A., Rahman, M.M., Rashid, S. and Garai, S. Synthesis and characterization of copper oxide nanoparticles: its influence on corn (Z. mays) and wheat (Triticum aestivum) plants by inoculation of Bacillus subtilis. *Environ. Sci. Pollut. Res. Int.* **2023**, 30(13), 37370-37385.

Haut, B., Halloin, V. and Amor, H.B. Development and analysis of a multifunctional reactor for equilibrium reactions: benzene hydrogenation and methanol synthesis. *Chem. Eng. Process.* **2004**, 43(8), 979-986.

He, H., Meyer, R.J., Rioux, R.M. and Janik, M.J. Catalyst design for selective hydrogenation of benzene to cyclohexene through density functional theory and microkinetic modeling. *ACS Catal.* **2021**, 11(19), 11831-11842.

Ishii, T., Kitamura, Y., Hasegawa, S., Sasaki, C., & Ozaki, J. I. Benzene hydrogenation activities of Ni catalyst supported on N-and B-doped carbons. *DRM.* **2021**, 119, 108550.

Jiang, H., Lu, S., Zhang, X., Peng, H. and Qiao, J. Preparation and application of a novel Raney nickel catalyst for fix-bed reactions. *Catal. Commun.* **2019**, 118, 60-64.

Jiang, L., Chu, G.W., Liu, Y.Z., Liu, W., Wen, L.X. and Luo, Y. Preparation of cordierite monolithic catalyst for α-methylstyrene hydrogenation in a rotating packed bed reactor. *Chem. Eng. Process.* **2020**, 150, 107882.

Kordulis, C., Lappas, A.A., Fountzoula, C., Drakaki, K., Lycourghiotis, A. and Vasalos, I.A. NiW/γ-Al_2O_3 catalysts prepared by modified equilibrium deposition filtration (MEDF) and non-dry impregnation (NDI): Characterization and catalytic activity evaluation for the production of low sulfur gasoline in an HDS pilot plant. *Appl. Catal. A Gen.* **2001**, 209(1-2), 85-95.

Kumar, K.D.A., Valanarasu, S., Ganesh, V., Shkir, M., AlFaify, S. and Algarni, H. Effect of potential voltages on key functional properties of transparent AZO thin films prepared by electrochemical deposition method for optoelectronic applications. *J. Mater. Res.* **2018**, 33(11), 1523-1533.

Li, T., Xia, D., Zhou, G., Xie, H., Jiao, Z. and Zhang, X. Effect of the morphology on the vapor phase benzene catalytic hydrogenation over Pd/CeO_2 catalyst. *Catal. Commun.* **2018**, 112 35–38.

Li, W.B., Zhuang, M., Xiao, T.C. and Green, M.L.H. MCM-41 supported Cu−Mn catalysts for catalytic oxidation of toluene at low temperatures. *J. Phys. Chem. B* **2006**, 110(43), 21568-21571.

Lin, Y.H. Biodegradation of 2, 4-Dichlorophenol by Mixed Culture in an Aerobic Fixed-Biofilm Process—Kinetic Model and Reactor Performance. *Environ. Eng. Sci.* **2015**, 32(6), 516-527.

Liu, J., Zhao, Z., Xu, C., Duan, A., Zhu, L. and Wang, X. Diesel soot oxidation over supported vanadium oxide and K-promoted vanadium oxide catalysts. *Appl. Catal.* **2005**, B, 61(1-2), 36-46.

Liu, Y., Gao, J., Liu, Q., Gu, F., Lu, X., Jia, L., Xu, G., Zhong, Z. and Su, F. Preparation of high-surface-area Ni/α-Al_2O_3 catalysts for improved CO methanation. *RSC Adv.* **2015**, 5(10), 7539-7546.

Liu, Y., Wang, Q., Wu, L., Long, Y., Li, J., Song, S. and Zhang, H. Tunable bimetallic Au–Pd/CeO_2 for semihydrogenation of phenylacetylene by ammonia borane. *Nanoscale Res. Lett.* **2019**, 11(27), 12932-12937.

Malins, K. and Malina, I. The effects of supported Pd, Pt, Re, Rh, Ru, Ir, Au, and Ni catalysts on renewable hydrocarbon production from alternative feedstock. *Biomass Bioenergy* **2023**, 171, 106732.

Manukyan, K.V., Cross, A.J., Yeghishyan, A.V., Rouvimov, S., Miller, J.J., Mukasyan, A.S. and Wolf, E.E. Highly stable Ni–Al_2O_3 catalyst prepared from a Ni–Al layered double hydroxide for ethanol decomposition toward hydrogen. *Appl. Catal. A Gen.* **2015**, 508, 37-44

Milone, C., Neri, G., Donato, A., Musolino, M.G. and Mercadante, L. Selective hydrogenation of benzene to cyclohexene on Ru/γ-Al_2O_3. *J. Catal.* **1996**, 159(2), 253-258.

Mohammadian, Z. and Parsafard, N. Optimization of Kinetic Study by Response Surface Methodology on the Various Types Ni Supported Catalysts in Competitive Benzene Hydrogenation. *Theor. Found. Chem. Eng.* **2022**, 56(6), 1179-1188.

Mohammadian, Z., Peyrovi, M.H. and Parsafard, N. Activity Evaluation of Ni-M (Ag, Cr and Mo) Supported on Zr-Containing Composites in Competitive Elimination of Benzene from Aromatic Mixture. *Silicon* **2020**, 12(8), 1943-1948.

Mohammadian, Z., Peyrovi, M.H. and Parsafard, N. Catalytic performance and kinetics study of various carbonaceous supported nickel nanoparticles for atmospheric pressure competitive hydrogenation of benzene. *Chem. Phys. Lett.* **2019**, 715, 367–374.

Mokrane, T., Boudjahem, A.G. and Bettahar, M. Benzene hydrogenation over alumina-supported nickel nanoparticles prepared by polyol method. *RSC Adv.* **2016**, 6(64), 59858-59864.

Molina, R. and Poncelet, G. Hydrogenation of benzene over alumina-supported nickel catalysts prepared from Ni (II) acetylacetonate. *J. Catal.* **2011**, 199(2), 162-170.

Mostafa, M.S., El Naga, A.O.A., Galhoum, A.A., Guibal, E. and Morshedy, A.S. A new route for the synthesis of self-acidified and granulated mesoporous alumina catalyst with superior Lewis acidity and its application in cumene conversion. *J. Mater. Sci.* **2019**, 54, 5424-5444.

Nedolivko, V. V., Zasypalov, G. O., Chudakov, Y. A., Vutolkina, A. V., Pimerzin, A. A., &Glotov, A. P. Effect of the ruthenium deposition method on the nanostructured catalyst activity in the deep hydrogenation of benzene. *Russ. Chem. Bull.* **2020**, 69, 260-264.

Ning, J., Xu, J., Liu, J. and Lu, F. Selective hydrogenation of benzene to cyclohexene over colloidal ruthenium catalyst stabilized by silica. *Catal. Letters* **2006**, 109(3-4), 175-180.

Oh, Y., Shin, J., Noh, H., Kim, C., Kim, Y.S., Lee, Y.K. and Lee, J.K. Selective hydrotreating and hydrocracking of FCC light cycle oil into high-value light aromatic hydrocarbons. *Appl. Catal. A: Gen.* **2019**, 577, 86-98.

Park, S., Abdullah, M.M., Seong, K. and Lee, S. Kinetic analysis of dibenzyltoluene hydrogenation on commercial Ru/Al_2O_3 catalyst for liquid organic hydrogen carrier. *J. Chem. Eng.* **2023**, 474, 145743.

Parsafard, N., Peyrovi, M.H. and Abdali Hajiabadi, M. Effect of textural properties of Ni (Nano)-supported catalysts on the selective benzene hydrogenation in the vapor phase. *Iran. J. Catal.* **2019**, 9(3), 241-249.

Parsafard, N., Peyrovi, M.H. and Abdali Hajiabadi, M. Nickel hydrogenation composite catalysts modified by zirconium in competitive benzene hydrogenation: Effect of modifiers. *Phys. Chem. Res.* **2020**, 8(2), 203-213.

Pawelec, B., Castaño, P., Arandes, J.M., Bilbao, J., Thomas, S., Peña, M.A. and Fierro, J.L.G. Factors influencing the thioresistance of nickel catalysts in aromatics hydrogenation. *Appl. Catal. A Gen.* **2007**, 317(1), 20-33.

Peyrovi, M.H., Parsafard, N. and Mohammadian, Z. Benzene selective hydrogenation over supported Ni (nano-) particles catalysts: Catalytic and kinetics studies. Chinese Journal of Chemical Engineering. *Chin. J. Chem. Eng.* **2018**, 26, 521–528.

Peyrovi, M.H., Rostamikia, T. and Parsafard, N. Competitive hydrogenation of benzene in reformate gasoline over Ni supported on SiO_2, SiO_2–Al_2O_3, and Al_2O_3 catalysts: influence of support nature. *Energ. Fuel* **2018**, 32(11), 11432-11439.

Rao, D., Xue, X., Cui, G., He, S., Xu, M., Bing, W., Shi, S. and Wei, M. Metal-acid site synergistic catalysis in Ru–ZrO_2 toward selective hydrogenation of benzene to cyclohexene. *Catal. Sci. Technol.* **2018**, 8(1), 236-243.

Ren, T.Z., Xu, P.B., Deng, Q.F. and Yuan, Z.Y. Mesoporous $Ce_{1-x}Mn_xO_2$ mixed oxides with CuO loading for the catalytic total oxidation of propane. *React. Kinet. Mech. Catal.* **2013**, 110, 405-420.

Rostamikia, T., Peyrovi, M. H., &Farajollahi, H. Study of the Effect of Catalyst Preparation Method on Benzene Reduction in the Refinery Platformate Using Competitive Hydrogenation. *Farayandno* **2019**, 13(64), 32-49.

Roy, S., & Datta, S. Hydrogenation of toluene on zirconium-modified hexagonal molecular sieve supported platinum and palladium catalysts. *Ind. Eng. Chem. Res.* **2013**, 52(49), 17360-17368.

Sassykova, L. R. Development of Catalysts for the Hydrogenation of the Aromatic Ring in Gasolines. *CABEQ* **2017**, 31(4), 447-453.

Savva, P.G., Goundani, K., Vakros, J., Bourikas, K., Fountzoula, C., Vattis, D., Lycourghiotis, A. and Kordulis, C. Benzene hydrogenation over Ni/Al_2O_3 catalysts prepared by conventional and sol–gel techniques. *Appl. Catal. B. Env.* **2008**, 79(3), 199-207.

Sharma, S., Agarwal, S. and Jain, A. Significance of hydrogen as economic and environmentally friendly fuel. *Energies* **2021**, 14(21), 7389.

Shubina, E. G., Filimonov, N. S., Shafigulin, R. V., Bulanova, A. V., Shishkovskii, I. V., & Morozov, Y. G. Effect of size of nickel nanoparticles on hydrogenation of benzene. *Pet. Chem.* **2017**, 57, 410-414.

Si, J., Guo, R., Zhang, Y., Ning, W., Sun, Y., Li, W. and Miao, S. Synthesis of Linde A-type zeolite from ball clay with incorporated ruthenium and application in hydrogenation catalysis. *Appl. Clay Sci.* **2023**, 239, 106897.

Sultana, M., Rownok, M.H., Sabrin, M., Rahaman, M.H. and Alam, S.N. A review on experimental chemically modified activated carbon to enhance dye and heavy metals adsorption. *Clean. Eng. Technol*. **2022**, 6, 100382.

Sun, H., Chen, Z., Li, C., Chen, L., Peng, Z., Liu, Z. and Liu, S. Selective hydrogenation of benzene to cyclohexene over Ru-Zn catalysts: Mechanism investigation on NaOH as a reaction additive. *Catal.* **2018**, 8(3), 104.

Tahir, N.A.M., Abdollah, M.F.B., Tamaldin, N., Zin, M.R.B.M. and Amiruddin, H. Optimisation of graphene grown from solid waste using CVD method. *J. Adv. Manuf. Technol.* **2020**, 106, 211-218.

Taleb, B., Jahjah, R., Cornu, D., Bechelany, M., Al Ajami, M., Kataya, G., Hijazi, A. and El-Dakdouki, M.H. Exploring Hydrogen Sources in Catalytic Transfer Hydrogenation: A Review of Unsaturated Compound Reduction. *Mol.* **2023**, 28(22), 7541.

Tang, C., Zhao, Y., Li, T., Liao, Z., Xu, B., Jiao, Z. and Zhou, G. Study of catalytic hydrogenation performance for the Pd/CeO_2 catalysts. International Journal of Chemical Reactor Engineering. *Int. J. Chem. React. Eng.* **2021**, 20(2): 251–259.

Tang, M., Huang, X., Peng, Y. and Lu, S. Hierarchical porous carbon as a highly efficient adsorbent for toluene and benzene. *Fuel* **2020**, 270, 117478.

Thiagarajan, S., Sanmugam, A. and Vikraman, D. Facile methodology of sol-gel synthesis for metal oxide nanostructures. *Rec. App. In sol-gel Syn.* **2017**, 1-17.

Wang, H., Yang, W., Tian, P., Zhou, J., Tang, R. and Wu, S. A highly active and anti-coking $Pd-Pt/SiO_2$ catalyst for catalytic combustion of toluene at low temperature. *Appl. Catal. A Gen.* **2017**, 529, 60-67.

Wang, L., Liu, Q., Jing, C., Yin, J., Mominou, N. and Li, S. Simultaneous removal of sulfides and benzene in FCC gasoline by in situ hydrogenation over $NiLaIn/ZrO_2$-r-Al_2O_3. *J. Hazard. Mater.* **2018**, 342, 758-769.

Wang, R., Zhang, M., Zhang, J. and Yang, J.H. Supported Nickel-based Catalysts for Heterogeneous Hydrogenation of Aromatics. *Chemistry Select* **2023**, 8(45), e202302787.

Wang, X., Shi, A., Duan, Y., Wang, J. and Shen, M. Catalytic performance and hydrothermal durability of CeO_2–V_2O_5–ZrO_2/WO_3–TiO_2 based NH_3-SCR catalysts. *Catal. Sci. Technol.* **2012**, 2(7), 1386-1395.

Wu, H.C., Chang, Y.C., Wu, J.H., Lin, J.H., Lin, I.K. and Chen, C.S. Methanation of CO_2 and reverse water gas shift reactions on Ni/SiO_2 catalysts: the influence of particle size on selectivity and reaction pathway. *Catal. Sci. Technol.* **2015**, 5(8), 4154-4163.

Xiao, Z., Zhang, Q., Chen, T., Cai, C., Ge, Q., Nie, Y., Ji, J. and Mao, J. Nickel–Tungsten Supported on Thin Carbon Coated SiO_2 Nanosphere for Cellulose Conversion to Lower Polyols. *Catal. Letters* **2018**, 148, 3757-3770.

Xue, X., Liu, J., Rao, D., Xu, S., Bing, W., Wang, B., He, S. and Wei, M. Double-active site synergistic catalysis in Ru–TiO_2 toward benzene hydrogenation to cyclohexene with largely enhanced selectivity. *Catal. Sci. Technol.* **2017**, 7(3), 650-657.

Yang, J.S., Jung, W.Y., Lee, G.D., Park, S.S., Jeong, E.D., Kim, H.G. and Hong, S.S. Catalytic combustion of benzene over metal oxides supported on SBA-15. *J. Ind. Eng. Chem*. **2008**, 14(6), 779-784.

Yao, X., Tang, C., Gao, F. and Dong, L. Research progress on the catalytic elimination of atmospheric molecular contaminants over supported metal-oxide catalysts. *Catal. Sci. Technol.* **2014**, 4(9), 2814-2829.

Ye, G., Sun, Y., Zhou, X., Zhu, K., Zhou, J. and Coppens, M.O. Method for generating pore networks in porous particles of arbitrary shape, and its application to catalytic hydrogenation of benzene. *J. Chem. Eng.* **2017**, 329 56–65.

Yu, X.L., Li, Y., Xin, S.M., Yuan, P.Q. and Yuan, W.K. Partial Hydrogenation of Benzene to Cyclohexene on Ru/XO_2 (X=Ti, Zr, or Si). *Ind. Eng. Chem. Res.* **2018**, 57(6), 1961-1967.

Zhang, Z., Zhu, Y., Asakura, H., Zhang, B., Zhang, J., Zhou, M., Han, Y., Tanaka, T., Wang, A., Zhang, T. and Yan, N. Thermally stable single atom $Pt/m\text{-}Al_2O_3$ for selective hydrogenation and CO oxidation. *Nat. Commun.* **2017**, 8(1), 16100.

Zhou, X., Yan, H., Feng, X., Zhao, H., Liu, Y., Chen, X. and Yang, C. Enhancing the conversion of polycyclic aromatic hydrocarbons from naphthenic heavy oil: novel process design, comparative techno-economic analysis, and life cycle assessment. *Ind. Eng. Chem. Res.* **2020**, 59(45), 20086-20101.

Zhu, Z.H., Radovic, L.R. and Lu, G.Q. Effects of acid treatments of carbon on N_2O and NO reduction by carbon-supported copper catalysts. *Carbon* **2000**, 38(3), 451-464.

APPENDIX A

A.1. BET Data

Table.5. Data from BET instrument

Relative Pressure (P/P_0)	Volume adsorbed (cm^3/g)	$1/[W((P/P_0) - 1)]$
0.0390421	4.8926	6.6442
0.0495688	5.1361	8.1248
0.100430	5.8990	15.143
0.150986	6.4830	21.949
0.20098	7.0246	28.638
0.25057	7.5450	35.456
0.300085	8.0743	42.487
0.319882	8.2911	45.389
0.993609	35.0560	3548.2
0.898720	32.8040	216.44
0.798063	28.7063	110.15
0.699740	19.0535	97.863
0.599111	13.2412	90.305
0.498356	10.5611	75.265
0.395895	9.0082	58.208
0.298013	7.8339	43.360
0.196851	6.7059	29.244
0.0964936	5.5699	15.342

A.2. Data of Power Law Model

Table.6. Values of reaction rate of H_2 and benzene, from which order of H_2 and benzene is calculated using Power Law Model

r_{H_2}	n_{H_2}	r_{Bz}	n_{Bz}
0.224	1.8	0.199	1.7
0.359	1.4	0.354	1.4
0.384	1.2	0.311	1.2
0.352	1.1	0.265	1.0
0.343	1.0	0.196	0.8

A.3. Data of Arrhenius Plot

Table.7. Data for lnk and 1/T to estimate the slope and intercept from the graph and temperature varies from 270^0-390^0C

lnk	$\frac{1}{T}$ (K^{-1})
-7.0355	0.00184
-5.24	0.00174
-4.448	0.00165
-5.403	0.00157

APPENDIX B

B.1. Calculation of different weight percentage catalyst

Nickel nitrate hexahydrate- $Ni(NO_3)_2 . 6H_2O$

Molecular weight of Ni = 58.69 g/mol

Molecular weight of N = 14.0067 gmol

Molecular weight of O = 16 g/mol

Molecular weight of H = 1.007 g/mol

So, molecular weight of $Ni(NO_3)_2 . 6H_2O$ = 58.69 + 2 × (14.0067 + 48) + 6 × (2 + 16) = 290.81 g/mol

Gram of $Ni(NO_3)_2 . 6H_2O$ required to prepare (2 wt%)Ni/ γ-Al_2O_3

58.61 g/mol of Ni contained in 290.81 g/mol of Ni salt

1 g/mol of Ni contained in $(\frac{290.81}{58.69})$ g/mol of Ni salt

So, to prepare (2 wt%)Ni/ γ-Al_2O_3 = $(\frac{290.81}{58.69} \times 2)$ = 14.86 g of Ni salt is required.

B.2. Surface area calculation using BET equation

$$\frac{p}{V(p_0 - p)} = \frac{1}{V_m.c} + \frac{c-1}{V_m.c}\frac{p}{p_0}$$

represents the form of,

Y = mx + C. where, $Y = \frac{p}{V(p_0 - p)}$, $x = \frac{p}{p_0}$, $m = \frac{c-1}{V_m.c}$ and, $C = \frac{1}{V_m.c}$

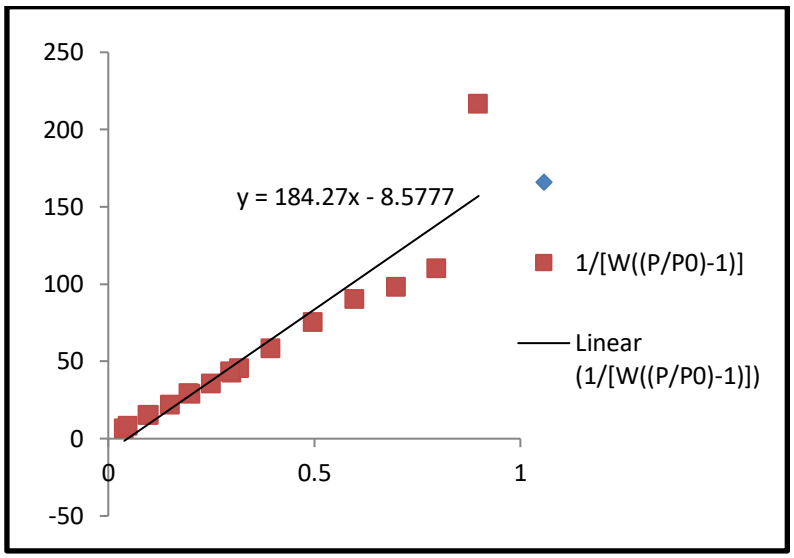


Fig.33. $\frac{p}{V\,(p_0 - p)}$ vs $\frac{p}{p_0}$ plot to determine slope and intercept

From the above linear graph,

Slope (m) = 184.27, and intercept (C) = -8.5777

So,

$$V_m = \frac{1}{(\text{Slope}+\text{Intercept})} = \frac{1}{(184.27-8.5777)} = 0.0056917 \text{ cm}^3/\text{g}$$

and,

$$S_T = \frac{V_m \,.\, N \,.\, S}{v} \text{ m}^2$$

or, $S_T = \frac{0.0056917 \times 6.023\times10^{23} \times 0.162 \times10^{-18}}{22.4}$

or, $S_{BET} = \frac{21.22024}{0.856} = 24.79 \text{ m}^2/\text{g}$

where, $S_{BET} = \frac{S_T}{a}$

V_m = monolayer volume in cm^3, N = Avogadro's No. (6.023×10^{23}), S = Cross-sectional area of a N_2 molecule (0.162 nm^2), v = molar volume of N_2 (22.4 L), V = amount of liquid N_2 adsorbed in cm^3/g of catalyst, p = vapour pressure of N_2 on the surface of material, p_0 = Pressure at STP 1 atm or 760 mmHg, c = BET constant, S_T = total surface area (m^2), S_{BET} = BET surface area of the material (m^2/g)

B.3. Calculation of activation energy

We know,

$r_i = \frac{X_i.F}{W_{cat}}$ and, $r_i = k.C_A$ (1^{st} order assumption) ; $C_A = C_{A_0}.(1 - X_i)$

where, X_i = conversion of benzene (%), F = flow rate of feed benzene (gmol/min), Wcat = weight of catalyst (g)

C_{A_0} = initial concentration of benzene (considering 8 mL flow rate volume) = $\frac{0.089}{0.008}$ = 11.125 gmol/L.

Now, to determine activation energy (E_a), we go for the expression,

$\ln k = \ln A - \frac{E_a}{RT}$

Determination of k_1

$r_i = \frac{(0.55 \times 0.089)}{11}$ = 0.00445 and X_1 = 0.55

or, $0.00445 = k_1 \times 11.125 \times (1 - 0.55)$

or, $k_1 = \frac{0.00445}{11.125 \times (1 - 0.55)}$

or, $k_1 = 0.00088\ min^{-1}$

Determination of k_2

$r_i = \frac{(0.88 \times 0.089)}{11}$ = 0.00712 and X_2 = 0.88

or, $0.00712 = k_1 \times 11.125 \times (1 - 0.88)$

or, $k_2 = \frac{0.00712}{11.125 \times (1 - 0.88)}$

or, $k_2 = 0.00533\ min^{-1}$

Determination of k_3

$r_i = \frac{(0.9416 \times 0.089)}{11} = 0.007618$ and $X_3 = 0.9416$

or, $0.007618 = k_3 \times 11.125 \times (1 - 0.55)$

or, $k_1 = \frac{0.007618}{11.125 \times (1 - 0.9416)}$

or, $k_1 = 0.01172\ min^{-1}$

Determination of k_4

$r_i = \frac{(0.8626 \times 0.089)}{11} = 0.006979$ and $X_4 = 0.8626$

or, $0.006979 = k_1 \times 11.125 \times (1 - 0.8626)$

or, $k_4 = \frac{0.006979}{11.125 \times (1 - 0.8626)}$

or, $k_4 = 0.00456\ min^{-1}$

lnk	$\frac{1}{T}$ **(K^{-1})**
-7.0355	0.00184
-5.24	0.00174
-4.448	0.00165
-5.403	0.00157

Slope $(-\frac{E_a}{R}) = -2779.8$ K

or, Ea = (2779.8 × 8.314) J/mol

or, Ea = 23111.25 J/mol = 23.11 kJ/mol.

B.4. Calculation of order for H_2 and benzene using Power Law Model

Considering, T=390^{0}C, k=0.0117 min^{-1} (optimum value is taken, gives the maximum conversion of benzene) and, lnk = -4.448

To determine r_{H_2} and r_{Bz}, the expression is

$$r = \frac{(\text{Bz flow rate} \times \text{Bz density} \times \text{Conversion})}{(\text{Mol.wt.of Bz} \times \text{Mass of catalyst} \times \text{Mass percentage of impregnated metal})}$$

To determine order for H_2 and benzene, the Power Law equation is used, $r = k.p_{H_2}^{n}.p_{Bz}^{m}$

Where, n = order of H_2

m = order of benzene

p_{H_2} = partial pressure of H_2 (bar)

p_{Bz} = partial pressure of benzene (bar). Since, the presence of H_2 gas is higher as compared to benzene so, the partial pressure effect is taken for H_2 gas only.

B.4.1. Determination of order for H_2

1st data point for r_{H_2} and $\ln p_{H_2}$

p_{H_2} = 5 bar and $\ln p_{H_2}$ = 1.609

$$(r_{H_2})_1 = \frac{(8 \times 0.8765 \times 0.55)}{(78 \times 11 \times 0.02)} = 0.224 \text{ mol/g.min}$$

and, $\ln r_{H_2} = n_1 \ln p_{H_2} + \ln k$

or, -1.496 = 1.609 n_1 – 4.448

or, n_{H_1} = 1.83

2nd data point for r_{H_2} and lnp_{H_2}

p_{H_2}= 10 bar and lnp_{H_2}= 2.302

$(r_{H_2})_2 = \frac{(8\times0.8765\times0.88)}{(78\times11\times0.02)}$ = 0.359 mol/g.min

and, $lnr_{H_2} = n_2\, lnp_{H_2} + lnk$

or, -1.024 = 2.302 n_2 – 4.448

or, n_{H_2} = 1.48

3rd data point for r_{H_2} and lnp_{H_2}

p_{H_2}= 15 bar and lnp_{H_2}= 2.708

$(r_{H_2})_3 = \frac{(8\times0.8765\times0.9416)}{(78\times11\times0.02)}$ = 0.384 mol/g.min

and, $lnr_{H_2} = n_3\, lnp_{H_2} + lnk$

or, -0.957 = 2.708 n_3 – 4.448

or, n_{H_3} =1.28

4th data point for r_{H_2} and lnp_{H_2}

p_{H_2}= 20 bar and lnp_{H_2}= 2.995

$(r_{H_2})_4 = \frac{(8\times0.8765\times0.8626)}{(78\times11\times0.02)}$ = 0.352 mol/g.min

and, $lnr_{H_2} = n_4\, lnp_{H_2} + lnk$

or, -1.044 = 2.995 n_4 – 4.448

or, n_{H_4} = 1.1

5th data point for r_{H_2} and lnp_{H_2}

p_{H_2}= 25 bar and lnp_{H_2}= 3.218

$(r_{H_2})_5 = \frac{(8\times0.8765\times0.8414)}{(78\times11\times0.02)}$ = 0.343 mol/g.min

and, $\ln r_{H_2} = n_5 \ln p_{H_2} + \ln k$

or, -1.07 = 3.218 n_5 – 4.448

or, n_{H_5} = 1.05

B.4.2. Determination of order for benzene

Since, the partial pressure of benzene (p_{Bz}) is not known in this study, we have considered change in conversion of benzene with respect to change in flow rate i.e., from LHSV curve. While conducting the experiment, we get maximum conversion of benzene at flow rate 8 mL/min using (2 wt%)Ni/γ-Al_2O_3 catalyst at T = 390^0C and P = 25 bar. So, we are keeping the flow rate of benzene (8 mL/min) constant while changing the conversion except 1st data point.

1st data point for r_{Bz} and $\ln p_{H_2}$

p_{H_2} = 5 bar and $\ln p_{H_2}$ = 1.609

$(r_{Bz})_1 = \frac{(4 \times 0.8765 \times 0.0.9748)}{(78 \times 11 \times 0.02)}$ = 0.343 mol/g.min

and, $\ln r_{Bz} = n_1 \ln p_{H_2} + \ln k$

or, -1.614 = 1.609 n_{Bz_1} – 4.448

or, n_{Bz_1} = 1.76

2nd data point for r_{Bz} and $\ln p_{H_2}$

p_{H_2} = 10 bar and $\ln p_{H_2}$ = 2.302

$(r_{Bz})_2 = \frac{(8 \times 0.8765 \times 0.0.8678)}{(78 \times 11 \times 0.02)}$ = 0.354 mol/g.min

and, $\ln r_{Bz} = n_2 \ln p_{H_2} + \ln k$

or, -1.038 = 2.302 n_{Bz_2} – 4.448

or, n_{Bz_2} = 1.48

3rd data point for r_{Bz} and lnp_{H_2}

p_{H_2}= 15 bar and lnp_{H_2}= 2.708

$(r_{Bz})_3 = \frac{(8\times0.8765\times0.0.7625)}{(78\times11\times0.02)}$ = 0.311 mol/g.min

and, $lnr_{Bz}= n_3 lnp_{H_2} + lnk$

or, -1.16 = 2.708 n_{Bz_3} – 4.448

or, n_{Bz_3} = 1.48

4th data point for r_{Bz} and lnp_{H_2}

p_{H_2}= 20 bar and lnp_{H_2}= 2.995

$(r_{Bz})_4 = \frac{(8\times0.8765\times0.0.65)}{(78\times11\times0.02)}$ = 0.265 mol/g.min

and, $lnr_{Bz}= n_4 lnp_{H_2} + lnk$

or, -1.328 = 2.995 n_{Bz_4} – 4.448

or, n_{Bz_4} = 1.04

5th data point for r_{Bz} and lnp_{H_2}

p_{H_2}= 25 bar and lnp_{H_2}= 3.218

$(r_{Bz})_5 = \frac{(8\times0.8765\times0.479}{(78\times11\times0.02)}$ = 0.196 mol/g.min

and, $lnr_{Bz}= n_5 lnp_{H_2} + lnk$

or, -1.629 = 3.218 n_{Bz_4} – 4.448 or, n_{Bz_5} = 0.87

APPENDIX C

IMAGES OF INSTRUMENTS AND CHEMICALS USED IN EXPERIMENT

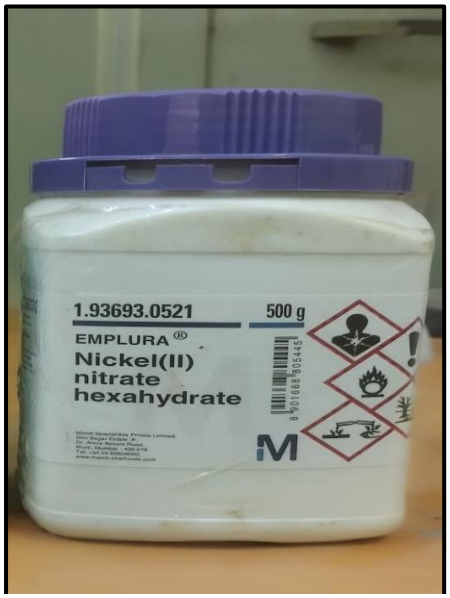


Fig.34. Precursor salt Nickel nitrate hexahydrate used for catalyst preparation

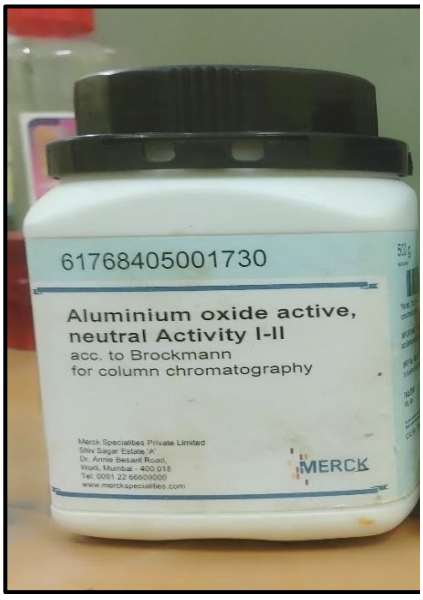


Fig.35. Support material alumina used for catalyst preparation

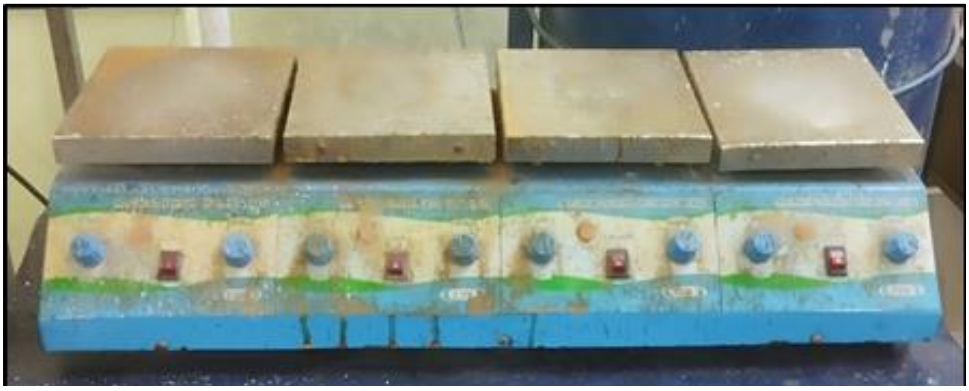


Fig.36. Magnetic stirrer with hot plate



Fig.37. Hot air oven instrument, used to dry the solution



Fig.38. Calcination chamber



Fig.39. Weigh machine for measuring precursor and support material

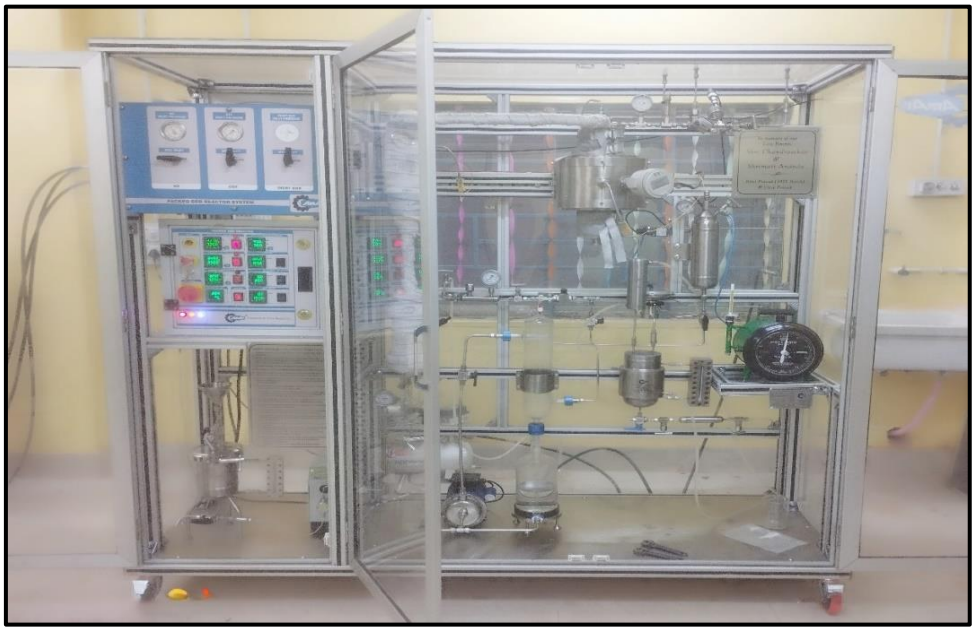


Fig.40. High pressure and high temperature catalytic fixed bed reactor used to study the hydrogenation reaction of benzene

BIODATA

Name: Arijit Saha

S/O: Kankana Saha

Address- 54/3/31J Debendra Chandra Dey Road, Tangra, Kol-700015

Educational Qualification

Secondary examination- 65% (2012)

Higher secondary examination- 65.8% (2014)

B.Tech in chemical engineering- 65.9% (2020)

M.E in chemical engineering- 88% (2024, June)